Dong *et al. Energy Mater.* **2025**, *5*, 500039
DOI: 10.20517/energymater.2024.194

Energy Materials

Review

Open Access

Catalyzed carbon-based materials for CO_2-battery utilization

Yulian Dong, Changfan Xu, Yonghuan Fu, Huaping Zhao, Yong Lei*

Fachgebiet Angewandte Nanophysik, Institut für Physik & IMN MacroNano, Technische Universität Ilmenau, Ilmenau 98693, Germany.

***Correspondence to:** Prof./Dr. Yong Lei, Fachgebiet Angewandte Nanophysik, Institut für Physik & IMN MacroNano, Technische Universität Ilmenau, Heisenbergbau 202, Unterpörlitzer Straße 38, Ilmenau 98693, Germany. E-mail: yong.lei@tu-ilmenau.de

How to cite this article: Dong, Y.; Xu, C.; Fu, Y.; Zhao, H.; Lei, Y. Catalyzed carbon-based materials for CO_2-battery utilization. *Energy Mater.* **2025**, *5*, 500039. https://dx.doi.org/10.20517/energymater.2024.194

Received: 27 Sep 2024 **First Decision:** 2 Dec 2024 **Revised:** 16 Dec 2024 **Accepted:** 27 Dec 2024 **Published:** 24 Jan 2025

Academic Editors: Yuhui Chen, Jiabao Yi **Copy Editor:** Fangling Lan **Production Editor:** Fangling Lan

Abstract

Increasing atmospheric CO_2 levels and global carbon neutrality goals have driven interest in technologies that both mitigate CO_2 emissions and provide sustainable energy storage solutions. Metal-carbon dioxide (M-CO_2) batteries offer significant promise due to their high energy density and potential to utilize atmospheric CO_2. A key challenge in advancing M-CO_2 batteries lies in optimizing CO_2-breathing cathodes, which are essential for CO_2 adsorption, diffusion, and conversion. Carbon-based cathodes play a critical role in facilitating CO_2 redox for M-CO_2 batteries, owing to their cost-effectiveness, high conductivity, tunable microstructure, and porosity. However, there is a lack of current systematic understanding of the relationship between the structure, composition, and catalytic properties of carbon-based cathodes, as well as their impact on the overall efficiency, stability, and durability of M-CO_2 batteries. In this review, we will give an insightful review and analysis of recent advances in various carbon-based materials, including commercial carbons, single-atom catalysts, transition metal/carbon composites, metal-organic frameworks, *etc.*, focusing on their structure-function-property relationships. A comprehensive understanding of the pivotal role played by carbon-based materials and their optimization strategies in M-CO_2 batteries will be provided. Moreover, future perspectives and research suggestions for carbon-based materials are presented to advance the development and innovation of M-CO_2 batteries.

Keywords: Carbon-based materials, electrocatalysts, CO_2 utilization, CO_2 batteries, CO_2 reduction reaction

INTRODUCTION

The global rise in atmospheric carbon dioxide (CO_2) levels has become an urgent environmental concern, necessitating sustainable carbon management strategies. Many countries have committed to carbon neutrality, setting ambitious targets to achieve net-zero emissions by mid-century[1-3]. For instance, the European Union aims for carbon neutrality by 2050, China by 2060, and the United States pledges a 50%-52% reduction in greenhouse gas emissions by 2030 compared to 2005 levels. Achieving these targets requires clean energy technologies, such as solar and wind power[4-6]. However, the intermittent nature of these energy sources, combined with growing energy demands, highlights the need for advanced energy storage systems to ensure a stable power supply.

Metal-carbon dioxide (M-CO_2) batteries represent a promising solution, utilizing CO_2 as a reactant for energy storage and offering high energy densities - up to 1,876 Wh/kg for Li-CO_2 and 1,125 Wh/kg for Na-CO_2 batteries[7-9]. These batteries address both CO_2 reduction and energy storage challenges, making them revolutionary for sustainable energy applications. Efficient CO_2-breathing cathodes are critical to their performance, facilitating CO_2 adsorption, diffusion, and conversion. Gas diffusion electrodes (GDEs), such as carbon paper or cloth, are commonly used to transport CO_2 to reaction sites, with electrocatalysts driving the conversion processes during charging and discharging[10-12]. Carbon-based materials are the leading candidates for M-CO_2 battery cathodes due to their low cost, high electrical conductivity, large surface area, and structural tunability. These materials can be engineered through doping, surface functionalization, and structural modifications to enhance their catalytic properties. However, challenges remain: commercial carbon materials, such as Ketjen Black (KB) and Super P, exhibit limited catalytic activity due to their inert nature and lack of active sites, as well as insufficient structural robustness to accommodate discharge products[13,14]; Single-atom catalysts (SACs), despite their high theoretical activity, are prone to forming agglomerated nanoparticles under operational conditions, leading to a loss of catalytic efficiency[15,16]; Transition metal/carbon composites often suffer from poor chemical and thermal stability, especially under high voltages and long-term cycling[17-19]; Similarly, metal-organic frameworks (MOFs), though offering high porosity and tunable structures, are susceptible to structural collapse or deactivation during catalytic processes, particularly in harsh electrochemical environments[20,21]. Addressing these limitations requires a deeper understanding of the interplay between structural and compositional properties and catalytic performance. The pore structure and surface area of carbon materials significantly influence CO_2 adsorption and diffusion[22], while functional groups or dopants can enhance catalytic activity by altering electronic structures. Robust carbon materials capable of withstanding high voltages, current densities, and long-term cycling are a major focus of research[7,23,24]. Similarly, interactions between carbon and transition metals in composite materials can enhance catalytic efficiency but require precise control of composition and nanostructures.

Despite progress in the field, a comprehensive analysis of the functional applications of carbon-based materials in M-CO_2 batteries remains lacking. This review aims to bridge that gap, providing a detailed examination of recent advancements in carbon-based cathode materials, their catalytic mechanisms, and functional applications. Strategies for enhancing catalytic efficiency, including innovative material designs and advanced fabrication techniques, will also be explored. By summarizing the relationships between material properties and battery performance, this review seeks to guide future research efforts and accelerate the commercialization of M-CO_2 batteries as a sustainable energy technology.

FUNDAMENTAL UNDERSTANDING OF M-CO_2 BATTERIES

Battery reaction mechanism

Electrochemistry of nonaqueous M-CO_2 batteries

A typical nonaqueous M-CO_2 battery consists of three main components: a metal anode, a porous CO_2-breathing cathode, and a separator containing a metal-ion-conducting electrolyte[25]. Figure 1A provides a schematic illustration of this configuration. Unlike the reversible insertion of Li^+ or Na^+ ions between the electrodes seen in traditional Li-ion or Na-ion batteries, the energy storage and release mechanism in M-CO_2 batteries is based on conversion reactions[26-29]. During discharge, the metal anode is oxidized, forming metal ions (M^{n+}, where n represents the oxidation state of metal ions), which then migrate through the organic electrolyte to the cathode. The movement direction of M^{n+} is indicated by the green arrow. Concurrently, CO_2 is reduced at the cathode, and the resulting reduction products react with the migrating metal ions to generate the final discharge product. This is referred to as the CO_2 reduction reaction (CO_2RR). During charging, the reactions reverse. When the battery is charged, the reverse occurs: discharge products are decomposed, releasing M^{n+} and CO_2, and the M^{n+} re-moves from the cathode to the anode (in the direction of the orange arrows), with metal being deposited back onto the anode and CO_2 evolving at the cathode. This process is commonly referred to as the CO_2 evolution reaction (CO_2ER)[30].

In nonaqueous M-CO_2 batteries, the CO_2RR can proceed *via* either a two-electron or a four-electron transfer pathway, resulting in distinct discharge products[7]. The two-electron transfer pathway typically leads to the formation of metal oxalate [$M_2(C_2O_4)_n$], while the four-electron transfer process yields a combination of metal carbonate and carbon as the discharge products. The mechanism involving the four-electron transfer pathway is now widely recognized, and the corresponding reaction equations can be summarized as follows: corresponding reactions can be expressed as follows:

Anodic reaction: $M \rightarrow M^{n+} + ne^-$

Cathodic reaction: $2CO_2 + 2e^- \rightarrow C_2O_4^{2-}$

$C_2O_4^{2-} \rightarrow CO_2^{2-} + CO_2$

$C_2O_4^{2-} + CO_2^{2-} \rightarrow 2CO_3^{2-} + C$

$CO_3^{2-} + 2\ M^{n+} \rightarrow M_2(CO_3)_n$

Overall reaction: $4\ M + 3CO_2 \leftrightarrow 2\ M_2(CO_3)_n + C$

Experimentally, significant progress has been achieved in understanding the electrochemistry of the four-electron transfer pathway in M-CO_2 batteries, and several physicochemical factors influencing the reaction mechanisms have been studied[31-33]. When studying intermediate discharge products, the intermediate $M_2(C_2O_4)_n$ is usually further converted to metal carbonate due to its poor thermal stability. Interestingly, it was discovered that under specific conditions, the intermediate product $C_2O_4^{2-}$ can be stabilized, implying that CO_2RR proceeds via the two-electron transfer pathway, and the corresponding reaction process is as follows:

$2\ M + 2CO_2 \leftrightarrow M_2(C_2O_4)_n$

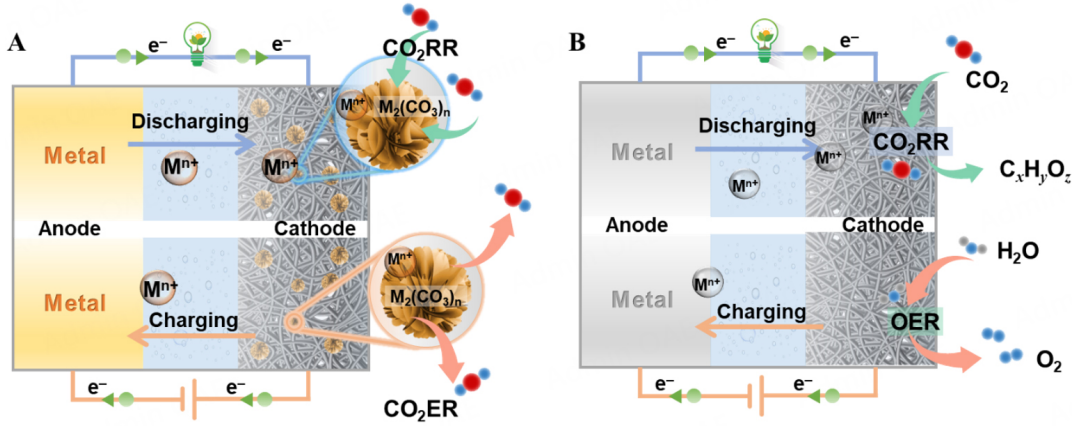

Figure 1. Schematic illustration of (A) Nonaqueous and (B) Aqueous M-CO_2 battery configuration.

For example, when using a molybdenum carbide (Mo_2C) catalyst, it was found that Mo_2C stabilizes the amorphous intermediate discharge product $Li_2C_2O_4$ through the delocalized electrons generated by Mo-O coupling[34,35]. Zhou *et al.* demonstrated that Mo-O chemical bonds form between Mo_2C and $C_2O_4^{2-}$ during discharge processes[36]. This interaction allows delocalized electrons from Mo^{2+} and Mo^{3+} in Mo_2C to transfer to the electronegative oxygen atoms in $C_2O_4^{2-}$, thereby stabilizing $Li_2C_2O_4$ as a discharge product. Notably, $Li_2C_2O_4$ decomposes thermodynamically more easily during charging (E° = 3.01 V *vs.* Li/Li^+) compared to Li_2CO_3 (E° = 3.82 V *vs.* Li/Li^+), reducing the charge potential to approximately 3.4 V. In contrast, catalysts such as carbon nanotubes (CNTs) lack this stabilization capability, causing $C_2O_4^{2-}$ to disproportionate into CO_3^{2-} and carbon, leading to the formation of Li_2CO_3, which is thermodynamically stable but highly insulating and difficult to decompose below 4.0 V. Furthermore, experimental results, including a precipitation test with $CaCl_2$ and H_3PO_4, confirm the presence of $C_2O_4^{2-}$ in Mo_2C-based systems but not in CNT-based systems. Density functional theory (DFT) calculations demonstrated the superior adsorption energy of Mo_2C for Li and CO_2, as well as its metallic conductivity and ability to stabilize $Li_2C_2O_4$. Charge density difference analyses further revealed significant electron transfer from Mo_2C to $Li_2C_2O_4$, unlike CNTs, which lack this capability. As a result, $Li_2C_2O_4$ forms as a stable discharge product with Mo_2C, while Li_2CO_3 is the primary discharge product for CNTs. Currently, few catalysts, including Mo_2C and MoN, have shown the ability to stabilize $M_2(C_2O_4)_n$. Enhancing interactions between Li^+ ions and electrolyte molecules also promotes the formation of stable solution-phase $C_2O_4^{2-}$ while suppressing the direct reduction of CO_2 to Li_2CO_3[37]. Thermodynamically, $M_2C_2O_4$ decomposes more readily than M_2CO_3, reducing charging voltage, facilitating reversibility, and enabling stable M-CO_2 battery operation[38-40]. DFT studies on Ru and Au catalysts in Li-CO_2 batteries further support this. $Li_2C_2O_4$ emerges as a kinetically favorable intermediate, with Li_2CO_3 as the thermodynamically stable product. Ru outperforms Au due to lower Gibbs free energy for nucleation and reduced activation barriers for rate-limiting steps, enabling efficient conversion of $Li_2C_2O_4$ into Li_2CO_3 and carbon along distinct reaction pathways[41].

Electrochemistry of aqueous M-CO_2 batteries

Aqueous M-CO_2 batteries are gaining particular attention due to their feature of simultaneously reducing CO_2 to value-added carbonaceous products and energy storage. As illustrated in Figure 1B, A typical aqueous M-CO_2 battery consists of a metal anode, a catalytically active cathode, and a separator (e.g., solid electrolyte for Li/Na-CO_2, or bipolar membrane for Zn/Al/Mg-CO_2 batteries) for separating the anolyte and catholyte. The main function of the anode chamber is to dissolve and deposit metals at the anode for energy release and storage during discharge and charging, respectively, similar to nonaqueous M-CO_2 batteries. The cathode chamber is similar to that of the electrolyzer of direct electrocatalytic CO_2 reduction, and thus

offers unique advantages for CO_2 conversion in the CO_2RR process based on the proton-coupled electron transfer mechanism that produces a wide range of carbon-containing products ($C_xH_yO_z$, such as HCOOH, CO, CH_4, CH_3OH, *etc.*), and the corresponding discharge reaction is as follows:

Anode: $M \rightarrow M^{n+} + ne^-$

Cathode: $CO_2 + H^+ + ne^- \rightarrow C_xH_yO_z$

Overall discharge reaction: $M + CO_2 + H^+ \rightarrow C_xH_yO_z + M^{n+}$

During the charging phase of aqueous M-CO_2 batteries, depending on the discharge product, the reaction may involve reversible conversion of the discharge product (mainly for HCOOH) or oxidation of H_2O [oxygen evolution reaction (OER)] (mainly for other difficult to oxidize products such as CO_2 or CH_4, *etc.*). The charging reaction can be expressed as follows:

Anode: $M^{n+} + ne^- \rightarrow M$

Cathode: $HCOOH \rightarrow CO_2 + 2H^+ + 2e^-$ or $2H_2O \rightarrow O_2(g) + 4H^+ + 4e^-$

Overall charging reaction: $M^{n+} + HCOOH \rightarrow CO_2 + H^+ + M$

or $M^{n+} + 2H_2O \rightarrow O_2 + 2M + 4H^+$

It is worth mentioning that (i) the fundamental difference between aqueous and nonaqueous M-CO_2 batteries lies in their reaction mechanisms, which are strongly influenced by the electrolyte environment. In nonaqueous M-CO_2 batteries, the reaction mechanism primarily involves the reduction of CO_2 to form solid discharge products such as $M_2(CO_3)_n + C$ or $M_2(C_2O_4)_n$. These solid products are decomposed reversibly during charging, releasing CO_2 again. In contrast, in aqueous M-CO_2 batteries, the reaction is more similar to direct electrocatalytic CO_2RR to produce carbon-containing products ($C_xH_yO_z$) due to the aqueous medium. Upon charging, oxidation of HCOOH or H_2O occurs depending on the type of discharge product.

(ii) Nonaqueous systems, typically composed of metal salts and solvents such as tetraethylene glycol dimethyl ether (TEGDME), leverage the low volatility, wide electrochemical window, and high chemical stability of ether-based electrolytes, making TEGDME a representative solvent widely used in nonaqueous M-CO_2 batteries[7,24]. In contrast, aqueous M-CO_2 batteries, such as Zn-CO_2 batteries, feature an alkaline anolyte [e.g., KOH mixed with $Zn(Ac)_2$] to promote Zn redox reactions and a near-neutral catholyte [e.g., $KHCO_3$ solution or $KHCO_3$ mixed with $Zn(Ac)_2$] to favor CO_2RR, as alkaline conditions conflict with CO_2RR pathways[42]. The two electrolytes are separated by a bipolar membrane to maintain their respective chemical environments, ensuring optimal reaction conditions at both electrodes.

(iii) The electrochemical performance of both nonaqueous and aqueous M-CO_2 batteries is heavily influenced by the properties of the cathode catalyst materials. In nonaqueous M-CO_2 batteries, $M_2(CO_3)_n + C$ is widely recognized as the main discharge product. However, it is found that under the influence of some special catalysts, the intermediate $M_2(C_2O_4)_n$ does not decompose further and can be stabilized while forming the final product. For example, when using a molybdenum carbide (Mo_2C) catalyst, it was found that Mo_2C stabilizes the amorphous intermediate discharge product $Li_2C_2O_4$ through the

delocalized electrons generated by Mo-O coupling[34]. Only a few reported catalysts (e.g., Mo_2C and MoN) have been able to stabilize the production of $M_2(C_2O_4)_n$. Therefore, catalysts that promote the stabilization of solid $M_2(C_2O_4)_n$ shall be preferred due to their high catalytic efficiency, and ability to stabilize intermediates. In addition, it is essential to develop catalysts that promote the reversible generation and decomposition of discharge products, such as $M_2(CO_3)_n$ + C. These catalysts can reduce charging polarization, thereby improving energy efficiency and prolonging battery life. For aqueous M-CO_2 batteries, catalysts that exhibit high selectivity and efficiency for CO_2 reduction to specific products are preferred. Examples include metal-based catalysts (e.g., Au and Ag) that can produce CO, and Sn-based catalysts that can produce HCOOH. Moreover, this catalyst needs to have OER catalytic activity to facilitate the charging reaction and reduce energy consumption.

Cathode engineering in CO_2-batteries

Fundamental challenges of cathode in M-CO_2 batteries

CO_2-breathing cathodes are the primary site of CO_2 capture, conversion, product formation, decomposition or release, involving multi-phase interfaces and complex reactions[18,43-46]. Typically, sufficiently efficient electron and mass (e.g., M^{n+} and CO_2) transfers and the abundance of catalytically active sites at the three-phase interface of the CO_2-breathing cathode are required to ensure that CO_2 is converted efficiently, so that the high performance of M-CO_2 batteries can be realized. Therefore, significant challenges arise and need to be addressed before their practical application [Figure 2].

(i) Limited CO_2 availability and utilization: ensuring a continuous and sufficient supply of CO_2 to the cathode is critical for the sustained operation of M-CO_2 batteries. However, the cathode structure (e.g., surface area, porosity, wettability, *etc.*) may be suboptimal, with uneven distribution of surface reaction sites, low reactivity, or a catalyst surface that is easily covered by products, making it difficult for CO_2 to adequately reach the reaction sites or to overflow before it has been reacted, leading to a lower efficiency of CO_2 utilization. Catalyst surfaces may also become blocked by discharge products, reducing access to active reaction sites. In aqueous systems, the hydrogen evolution reaction (HER) competes with CO_2RR[47,48], consuming energy and further decreasing CO_2 conversion efficiency due to the favorable reduction of H_2O to H_2 gas.

(ii) Sluggish reaction kinetics of CO_2RR: CO_2 is chemically stable, with a strong C=O bond (750 kJ mol^{-1}) necessitating high overpotentials for activation. The CO_2RR process involves multi-step electron transfers and the formation, dissolution, and adsorption of intermediates. Suboptimal interactions between the cathode material and these intermediates often lead to kinetic bottlenecks. Ideal cathode materials should effectively adsorb CO_2 and intermediates, facilitating their reduction while maintaining optimal binding strength.

(iii) Clogging of CO_2-breathing cathodes: in aqueous M-CO_2 batteries, the discharge products are dissolved in the electrolyte. However, in nonaqueous M-CO_2 batteries, insoluble carbonate discharge products (e.g., Li_2CO_3 and Na_2CO_3) precipitate on the cathode surface or within its pores, clogging channels and blocking CO_2 and ion diffusion. The limited solubility and low diffusivity of CO_2 in nonaqueous electrolytes exacerbate uneven product deposition, concentrating discharge products near the CO_2 source. This spatial imbalance leads to increased charge transfer resistance, higher overpotentials, and significant capacity decline over time, ultimately reducing battery lifespan and practical viability.

(iv) Cathode corrosion and degradation: high charging voltages required to decompose insulating carbonate products can cause undesirable side reactions, including electrolyte decomposition and cathode corrosion.

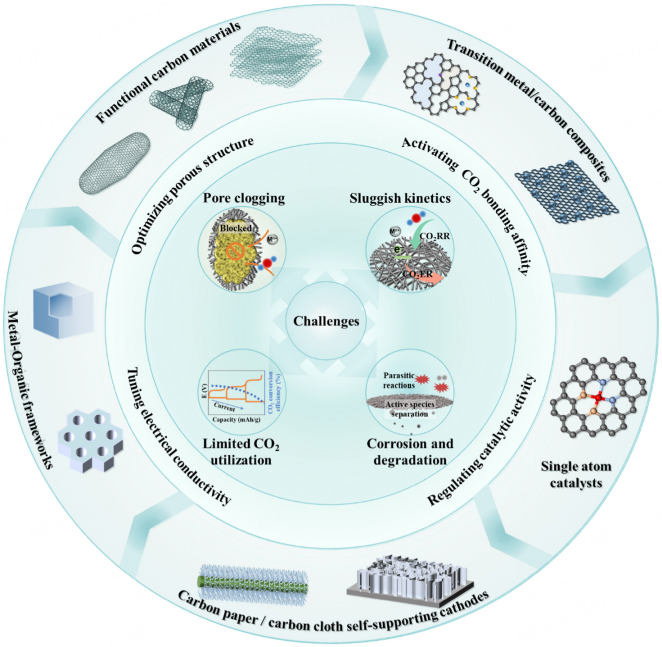

Figure 2. Challenges, structural design principles and typical carbon-based materials of CO_2-breathing cathodes for M-CO_2 batteries.

Carbon-based materials may corrode due to reactive oxygen species, while metal cathodes can form passivating oxides or hydroxides in the presence of H_2O, O_2 and CO_2. Repeated redox cycling can induce stress accumulation, microstructural changes, or crack formation, invalidating active sites and limiting performance. At the nanoscale, local electric fields and structural remodeling can further degrade the catalyst, diminishing system efficiency and durability.

Structural design of cathode in M-CO_2 batteries

To clearly address the aforementioned challenges, a well-designed CO_2-breathing cathode should fulfill several key functions, including facilitating the diffusion of M^{n+} ions and CO_2, catalyzing the formation and decomposition of the discharge products, providing sufficient storage space for these products, and guiding their morphological evolution. To meet these functional requirements, several critical performance metrics must be optimized: (i) High electrical conductivity and an optimized porous structure are key for CO_2 cathodes. Conductivity ensures fast electron transfer, reducing internal resistance and boosting power output. A well-designed porous structure helps diffuse Mn^+ ions and CO_2 and stores discharge products. Mesopores (2-50 nm) can facilitate CO_2 and ion transport, while macropores (> 50 nm) provide ample space for the storage of insulating discharge products such as Li_2CO_3 or Na_2CO_3, reducing impedance and enhancing cycle performance[49]. One study shows that combining micro- and mesopores increases surface area (2,003 *vs.* 1,813 m^2g^{-1}), enhancing ion and gas movement. However, excessive activation reagents can collapse the structure, reducing surface area. A balance between pore size and volume is crucial[50]. Therefore, a balance between pore size and volume is desirable; (ii) Favorable CO_2 bonding affinity. An ideal CO_2 cathode should possess a high binding affinity for CO_2 to facilitate its adsorption and activation, which helps reduce the energy barriers associated with CO_2RR, improving overall reaction kinetics and battery performance; and (iii) Excellent catalytic activity. To achieve high electrochemical performance, catalytic cathodes should possess abundant and accessible active sites for CO_2RR and CO_2ER, to lower the overpotential during both charge and discharge cycles, and to improve the overall efficiency of the battery. Whereas in aqueous M-CO_2 batteries, depending on their charging/discharging mechanism, effective CO_2RR/CO_2ER or CO_2RR/OER bifunctional electrocatalysts are required on the CO_2 cathode.

Importance and strategies of carbon-based cathode for M-CO_2 batteries

As mentioned earlier, the remarkable electrical conductivity, low mass density, affordability, significant specific surface area, customizable porous structure, and macroscopic morphology contribute to the extensive investigation of carbon materials in M-CO_2 batteries. For example, Super P and KB with inherent high conductivity have been widely recognized as conductive agents, which are essential for electron transfer in M-CO_2 batteries[14,45,51]. In addition, carbon materials (e.g., CNTs and graphene) have a tunable porous structure allowing for optimized pore size distribution and a large specific surface area, which contributes to the efficient adsorption of CO_2, thus ensuring the efficient diffusion of CO_2 and M^{n+} ions and providing space for the storage of discharge products. Additionally, carbon paper and carbon cloth serve as current collectors or gas diffusion layers, providing a conductive framework that allows for the efficient electron transfer from the external circuit to the active sites, while facilitating the diffusion of CO_2 into the catalyst and enhancing the supply of CO_2 at the active sites[52-54]. Consequently, the presence of carbon materials is indispensable in M-CO_2 batteries.

However, pure carbon materials have limited catalytic activity in promoting CO_2RR and CO_2ER processes, which may lead to higher overpotentials. Carbon materials alone may not be sufficient to achieve the high catalytic activity required for practical M-CO_2 batteries[55-57]. To overcome this limitation, various integrated strategies have been reported: (a) Nanostructure engineering to design conductive networks with hierarchical porous structures to alleviate pore clogging and promote sustained M^{n+} and CO_2 transport; (b) constructing of CO_2 cathodes with sufficient electrocatalytic activity, e.g., doping (e.g., heteroatom doping such as N, S, B, *etc.*), metal/carbon composites, single atom (SA) catalysts, MOFs or, to enhance their CO_2 bonding affinity and catalytic activity; and (c) designing self-supporting cathodes for surface protection of the carbon layer to mitigate the degradation of the carbon cathode.

CATALYZED CARBON-BASED MATERIALS IN CO_2-BATTERIES APPLICATION

In this section, our primary focus will be on exploring the application of carbon-based materials in M-CO_2 batteries, with an emphasis on their inherent advantages in achieving high-performance M-CO_2 batteries. The main objective is to gain a comprehensive understanding of how carbon materials with diverse microstructures, surface properties, and compositions contribute significantly to enhancing the electrochemical performance of M-CO_2 batteries. Furthermore, potential future research directions for improving M-CO_2 battery performance using carbon-based materials will be proposed.

Commercial carbon materials

Ketjen black and super P

Commercial carbon materials, such as KB and Super P, are widely used as cathode materials for M-CO_2 batteries due to their favorable electronic conductivity, large surface area, chemical stability, low cost, and scalable manufacturing processes. While Super P was among the first carbon materials used as a cathode in M-CO_2 batteries, the electrolyte plays a critical role in determining overall battery performance, even when the electrode materials remain the same. For instance, Ci *et al.* found that Super P had negligible discharge capacity in ionic liquid (IL) electrolytes[58]. In contrast, Yang *et al.* demonstrated significantly improved discharge capacity (6,062 mAh g^{-1}) in a Li-CO_2 battery using Super P with an ether-based electrolyte. This capacity further increased to 8,229 mAh g^{-1} with the addition of Ru metal (Ru@Super P)[59]. Similarly, Guo *et al.* developed a porous KB-supported Ru nanoparticle (Ru@KB) composite that enhances the decomposition of Na_2CO_3, lowering charge voltage and improving cycling performance in Na-CO_2 batteries[60]. With the Ru@KB cathode, the batteries achieved a high discharge capacity of 11,537 mAh g^{-1} and a Coulombic efficiency of 94.1%, and ran for over 130 cycles with stable performance[60]. The disparity in performance is attributed to the electrolyte's effect on the stability of intermediate discharge products and

the formation of final products. Early studies on Na-CO_2 batteries with Super P cathodes in different electrolytes confirmed this trend. However, their electrochemical performance is limited by inherent drawbacks, including low conductivity, small pore volume, and limited active sites.

Carbon nanotubes

Commercial CNTs, featuring a porous, cross-linked structure with 5 nm wall thickness and 0.34 nm interlayer spacing, are integral to M-CO_2 batteries. The outer CNT walls facilitate nucleation and anchoring of $M_2(CO_3)_n$ products, while inner walls enhance conductivity and electron transfer. Xiao *et al.* examined the discharge and charge behavior of Li-CO_2 batteries with CNT electrodes under varying current densities [Figure 3A][61]. Voltage profiles revealed two stages: an initial low-voltage plateau decreasing during charging and a sharp rise to completion [Figure 3B]. |dV/dQ| analysis identified three phases: rapid polarization (L0), characteristic peaks (L1), and stabilization (L2). Lower currents prolonged L1 but increased crystalline Li_2CO_3 formation, raising resistance and irreversibility. Pure CNT cathodes often exhibit high charging voltages and electrolyte decomposition[62]. However, multi-walled CNTs (MWCNTs) have demonstrated improved performance, such as a Li-CO_2 battery with Au nanoparticle-supported CNTs achieving 6,399 mAh g^{-1} at 100 mA g^{-1}[63]. Further advancements will be discussed in the next chapter.

Graphene

Graphene, with its excellent conductivity, large surface area, and high stability, is an ideal cathode material for Li-CO_2 batteries[64,65]. Its structure enables efficient oxygen diffusion, ample discharge product storage, and abundant active sites. Zhang *et al.* developed ultrathin, porous graphene nanosheets with enhanced electrolyte wettability and CO_2 diffusion, achieving discharge capacities of 14,722 and 6,600 mAh g^{-1}, with a stable 2.77 V plateau at 50 mA g^{-1}[66]. However, the efficiency and reaction kinetics of graphene-based cathodes remain moderate. Strategies such as heteroatom doping, defect engineering, and compositing with metals or non-metals are being explored to further boost the electrochemical performance of graphene in M-CO_2 batteries.

Defective carbon

Topological defects in carbon structures, such as pentagon and heptagon rings, create highly active sites for CO_2RR in Li-CO_2 batteries. Ye *et al.* developed defect-rich graphene (TDG) by removing nitrogen dopants from N-doped graphene at high temperatures, introducing topological defects [Figure 3C][67]. TDG-1000 exhibited a high surface area (410 m^2 g^{-1}) and porous structure, enhancing electrolyte and CO_2 contact, Li-ion transport, and product absorption. As an air cathode, TDG-1000 achieved a discharge capacity exceeding 69,000 mAh g^{-1} at 0.5 A g^{-1}, low overpotential (1.87 V) at 2 A g^{-1}, and stable cycling for 600 cycles at 1 A g^{-1} [Figure 3D and E]. Both DFT and experiments highlighted that topological defects outperform conventional N-doped sites in Li-CO_2 batteries[67].

Heteroatom doped carbon

Doping involves introducing non-metal atoms or different metal ions into the carbon-based structure to modify its properties, including structure, electrochemical behavior, and electrocatalytic activity. Heteroatom doping adjusts the Fermi level and electronic structure of the carbon-based material, influencing adsorption energy, adsorption modes, and material interface properties, thereby enhancing gas reduction kinetics. Additionally, heteroatom doping stabilizes the structure, creates abundant active sites, and improves the inherent conductivity of the carbon-based material, which facilitates the decomposition of M-CO_2 discharge products. Consequently, doping with heteroatoms such as B, N, S, P, and F is a proven strategy for enhancing the catalytic activity of carbon-based material in M-CO_2 batteries.

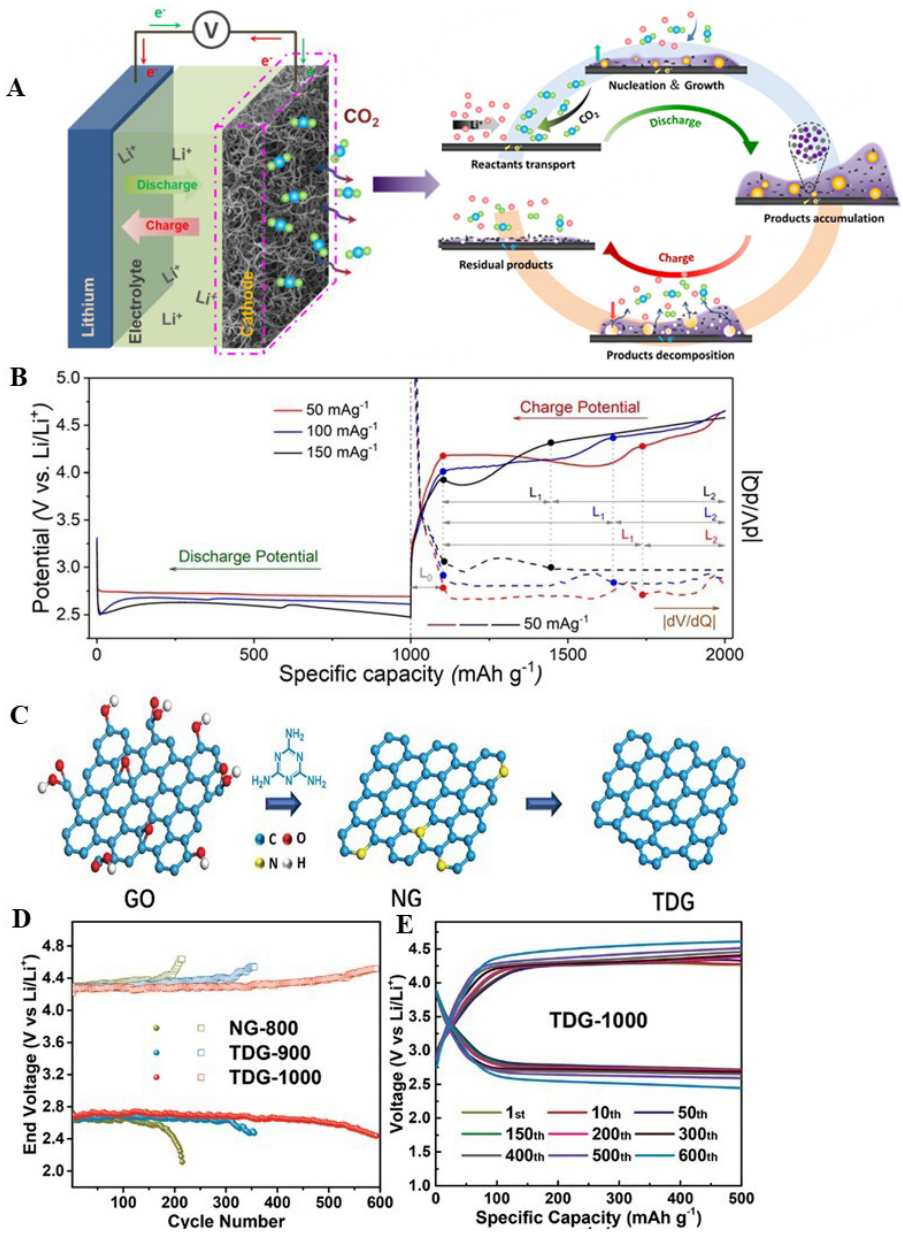

Figure 3. (A and B) Discharge/charge mechanisms and performances of Li-CO_2 batteries with CNT electrodes[61]. (C) Preparation of NG and TDG and (D and E) long-term cycling performances and stability[67]. These figures are reproduced with permission from American Chemical Society[61] and Wiley[67], respectively.

N-doped carbon

Nitrogen doping significantly enhances the CO_2RR in carbon-based materials by disrupting charge neutrality and redistributing electrons, imparting unique catalytic properties. The synthesis methods and precursor materials play a pivotal role in modulating heteroatom dopants. Common approaches for N-doped carbon catalysts include: (i) etching carbon with nitrogen sources such as NH_3; (ii) pyrolytic conversion of nitrogen-rich precursors such as MOFs or polymers; and (iii) *in situ* growth from nitrogen-containing gaseous species[68-70]. Among nitrogen configurations, pyridinic-N and pyrrolic-N exhibit superior catalytic performance in CO_2RR and CO_2ER compared to graphitic-N, due to stronger interactions with CO_2 and Li that enhance adsorption and reaction kinetics[71-73]. These active nitrogen species contribute

to electronic affinity, wettability, and catalytic activity, while graphitic-N improves electrical conductivity, facilitating charge transport[74]. Thus, optimizing catalysts with a high content of pyridinic- and pyrrolic-N alongside good conductivity is essential for enhanced performance[75]. Chen *et al.* activated nitrogen (N)-doped graphene with CO_2, achieving 72.65% pyridinic- and pyrrolic-N content, which enabled reversible Li_2CO_3 transformation in Li-CO_2 batteries[76]. This resulted in a low voltage gap of 2.13 V at 1,200 mA g^{-1} and excellent cycling stability over 170 cycles at 500 mA g^{-1}. Additionally, K-CO_2 batteries with N-doped CNT (NCNT) cathodes and KF-rich solid electrolyte interphase (SEI)-protected K anodes achieved 9,436 mAh g^{-1}, capacity, a 0.81 V overpotential gap at 50 mA g^{-1}, and 450 cycles. Fiber-shaped batteries also demonstrated stable power output under bending conditions, highlighting their flexibility and potential for next-generation energy storage[77]. These advancements emphasize nitrogen doping as a crucial strategy for optimizing M-CO_2 battery performance.

N, S co-doped carbon

Carbon and sulfur (S), both p-block elements, share similar electronic structures with p-orbital outer electrons. However, the higher electronegativity of sulfur enables stronger electron attraction and interactions with atoms and functional groups, making S-doped carbon nanomaterials highly attractive for catalysis. Sulfur also acts as a bridge, inducing coupling effects that form robust carbon-based composites[78-80]. Recently, introducing N and S heteroatoms in carbon catalysts has emerged as a strategy to modulate p-band centers, optimize orbital hybridization, and accelerate CO_2RR and CO_2ER kinetics[81-84]. Wang *et al.* demonstrated the vertical growth of an N, S co-doped porous carbon (NS-PC) network on self-supporting carbon paper using salt-template and vacuum-sealed sulfurization methods, guided by DFT calculations[85]. This two-step synthesis reduced formation energy and yielded a high concentration of dopants [Figure 4A and B]. The study revealed that the NS-PC exhibited a moderate p-band center, resulting in superior CO_2RR and CO_2ER kinetics. The N, S co-doped graphene (NS-G) catalyst, with its moderate p-band center, exhibited the highest CO_2ER catalytic activity [Figure 4C]. Weak adsorption causes premature Na_2CO_3 desorption, while overly strong adsorption increases the energy barrier for Na-O bond dissociation [Figure 4D]. This balance enabled highly reversible formation and decomposition of Na_2CO_3 and carbon, resulting in excellent cycling stability over 1,000 h at 10 μA cm^{-2}, a low 1.04 V voltage gap, and 71.2% energy efficiency. Moreover, N, S-doped CNTs combined with flexible gel electrolytes have demonstrated superior performance in quasi-solid, flexible planar Li-CO_2 batteries. These systems omit traditional separators, enhancing the reversible formation and decomposition of Na_2CO_3 for improved efficiency and stability[86].

N, B co-doped carbon

Additionally, N and boron (B) co-doped porous graphene has been investigated as a bifunctional metal-free cathode catalyst for rechargeable Li-CO_2 batteries[87]. For example, Qie *et al.* developed a novel B, N co-doped porous graphene (BN-hG), which serves as an efficient bifunctional cathode catalyst for rechargeable Li-CO_2 batteries[87]. Due to the unique porous nanostructure and high catalytic activity of the BN-hG catalyst, the newly developed Li-CO_2 battery exhibits low polarization, excellent rate performance, and exceptional long-term cycling stability, achieving 200 cycles at a current density of 1.0 A g^{-1}. Recently, Kaur *et al.* developed a tubular B, N co-doped nanotubes-like material (C-BN@600), as shown in Figure 4E and F, from an IL and MOF composite[88]. The C-BN@600 catalyst efficiently reduces CO_2 to methanol with a 74% Faradaic efficiency and a production rate of 2,665 μg h^{-1} mg^{-1}, driven by the synergistic effects of B and N co-doping that enhance catalytic sites. DFT calculations revealed that B and N play distinct roles: B acts as an electron-withdrawing site, and N as an electron-donating site, together improving the adsorption of intermediates necessary for methanol formation, Figure 4G[88]. When used in a Zn-CO_2 battery, the system delivered a power density of 5.42 mW cm^{-2} and an energy density of 330 Wh kg^{-1}, while operating stably for over 12 days and 800 cycles [Figure 4H].

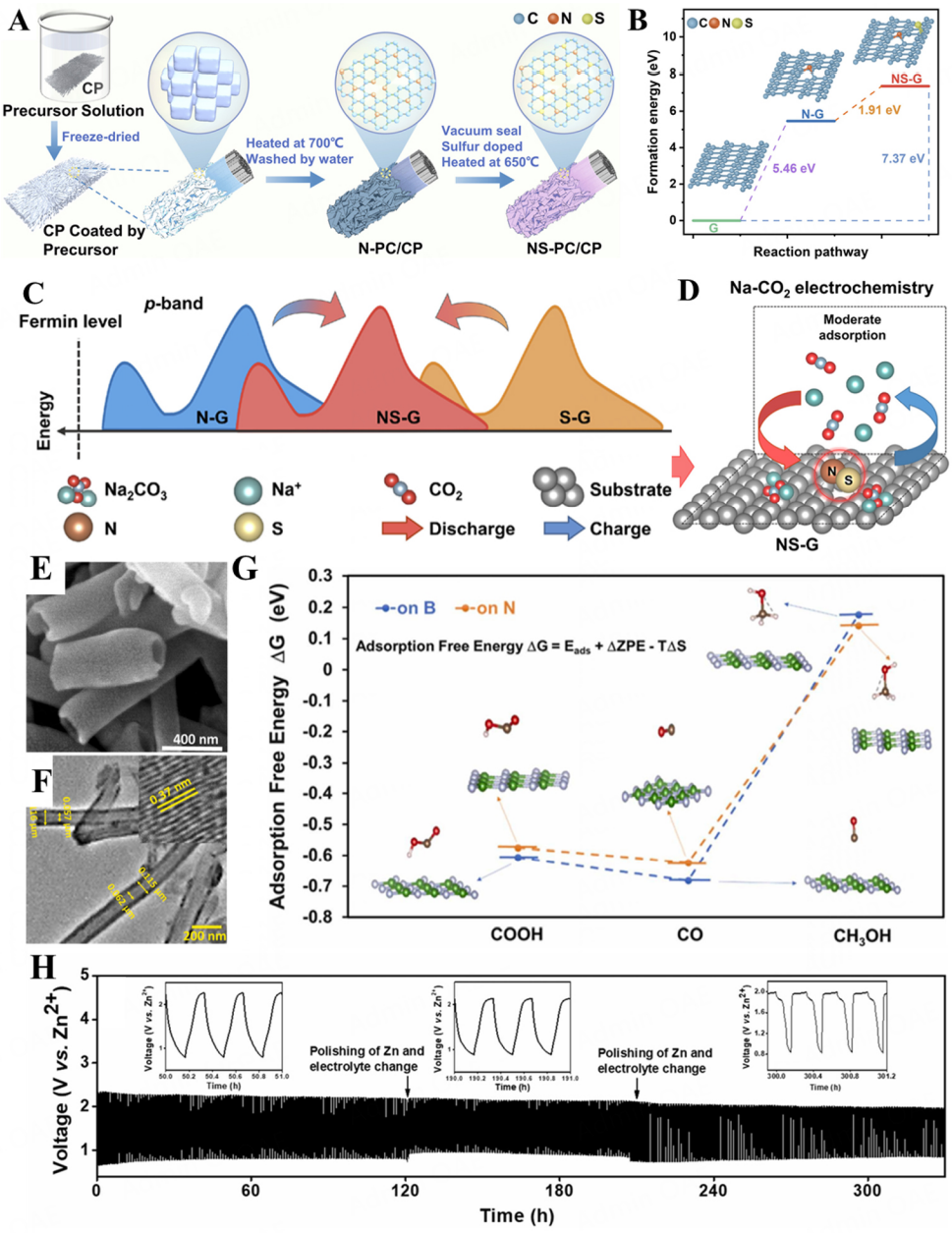

Figure 4. (A) Synthesis of NS-PC/CP, (B) Formation energies of NS-G. (C) Illustration of p-band center design and (D) the CO_2RR kinetics on NS-G catalysts[85]. (E) FE-SEM and (F) HR-TEM images of C-BN@600. (G) Reaction coordinates for CO_2 reduction on BN[88]. (H) Electrochemical performance. These figures are reproduced with permission from Elsevier[85,88].

Transition metal/carbon composites

Based on recent advancements in M-CO_2 batteries, transition metal/carbon composites, encompassing both noble and non-noble metal/carbon composites, have emerged as promising catalysts, offering significant improvements in performance and cost-efficiency. Noble metal/carbon composites, such as Pt/C or Pd/C, benefit from the exceptional catalytic activity and stability of noble metals, while the carbon matrix maximizes the exposure of active sites, enhancing efficiency[18,89,90]. The high cost of noble metals necessitates

alternatives such as non-noble metal/carbon composites (e.g., Fe, Co, and Ni), which offer comparable catalytic performance, better stability under harsh conditions, and lower costs. These materials leverage tunable electronic structures and strong metal-carbon interactions. However, challenges remain in enhancing non-noble metal efficiency, developing scalable synthesis methods, and ensuring long-term stability. Addressing these issues is vital for advancing transition metal/carbon composites in M-CO_2 battery technologies.

Noble metal/carbon composites

Ru catalysts offer a cost advantage among platinum group metals, being the least expensive. Their highly tunable electronic structure and unfilled $4d^7$ orbitals enable superior electrocatalytic activity for CO_2RR[40,91,92]. For instance, Qiao *et al.* demonstrated that in Li-CO_2 batteries, Ru enables both Li_2CO_3 and carbon to undergo reversible decomposition ($2Li_2CO_3 + C \rightarrow 2CO_2 + 4Li^+ + 4e^-$, $E^\circ = 2.8$ V *vs.* Li/Li^+), overcoming the 3.82 V thermodynamic limit observed with Au catalysts ($2Li_2CO_3 \rightarrow 2CO_2 + O_2 + 4Li^+ + 4e^-$, $E^\circ = 3.82$ V *vs.* Li/Li^+), where carbon is nearly impossible to decompose[93]. This is attributed to the catalytic activity of specific Ru crystal facets, which lower reaction barriers and promote reversibility. While the precise catalytic mechanisms of Ru remain partially unclear, its superior performance and economic feasibility have made it a focus of research. Ru AC + SA@NCB integrates Ru clusters (Ru AC) and Ru-N_4 sites, improving carbon desorption, preventing poisoning, and accelerating discharge voltage[94]. This synergy reduces energy barriers, achieving high rates with low overpotentials. In M-CO_2 batteries, Ru catalysts are often combined with or supported by carbon materials[7,95,96]. Atomically dispersed Ru anchored on Co_3O_4 nanosheets supported by carbon cloth (SA Ru-Co_3O_4/CC) forms bifunctional catalysts[97]. This combination provides high electrical conductivity, large surface areas, and well-structured porosity, which are critical for enhancing CO_2 diffusion, ion transport, and uniform Ru distribution. These properties maximize catalytic efficiency while functional groups on the carbon surface interact with Ru, further stabilizing active catalytic sites and enhancing the catalyst's performance. In addition to the excellent catalytic activity of metallic Ru, its oxide, RuO_2, also demonstrates significant catalytic capabilities for reversible M-CO_2 batteries. In our previous work, as depicted in Figure 5A, we developed RuO_2 nanoparticles coated on carbon paper (RuCP) for Na-CO_2 batteries[98]. Hydrous $RuO_xN_yS_z$ was deposited onto pretreated carbon paper and annealed in nitrogen, producing highly dispersed RuO_2 nanoparticles within a 3D carbon matrix. This design enhances structural stability, promotes sodium nucleation, and improves CO_2RR and CO_2ER kinetics[98].

Other noble metals, such as Pt, Ir, Au, and Pd, along with their oxides, have also shown promise as effective bifunctional catalysts for M-CO_2 batteries, warranting further exploration[99-101]. Chen *et al.* advanced this further by engineering a porous Pt-(111)@CC catalyst using electro-joule heating. Its (111) crystal orientation improved CO_2 conversion kinetics and catalytic activity [Figure 5B and C][99]. The catalyst exhibited an exceptionally low overpotential (0.45 V) and high stability over 200 cycles, doubling area-specific capacity. A stacked Li-CO_2 pouch cell incorporating this catalyst demonstrated stable cycling at 20 μA cm^{-2} with a low overpotential (0.5 V) and 82.2% energy efficiency, as shown in Figure 5D-F. Compared to prior designs, this porous Pt-based cell showcased superior stability and scalability, highlighting its potential for large-scale applications[99]. A Pt-N-doped polypyrrole (NPPy)-CNT composite by synthesizing NCNTs (NPPy-CNTs) and depositing Pt nanoparticles via magnetron sputtering was developed by Chen *et al.*[102]. This cathode catalyst delivered a high discharge capacity of 29,614 mAh g^{-1} with a low overpotential (0.75 V) and stable cycling over 30 cycles. N-doping enhanced conductivity and catalytic activity by creating defects and active sites, while uniform Pt dispersion facilitated Li_2CO_3 decomposition during charging, boosting performance and reversibility[102]. Zhang *et al.* designed a Pt/FeNC catalyst for Li-CO_2/O_2 batteries by dispersing 2.4 nm Pt nanoparticles onto porous FeNC microcubic supports[103]. This

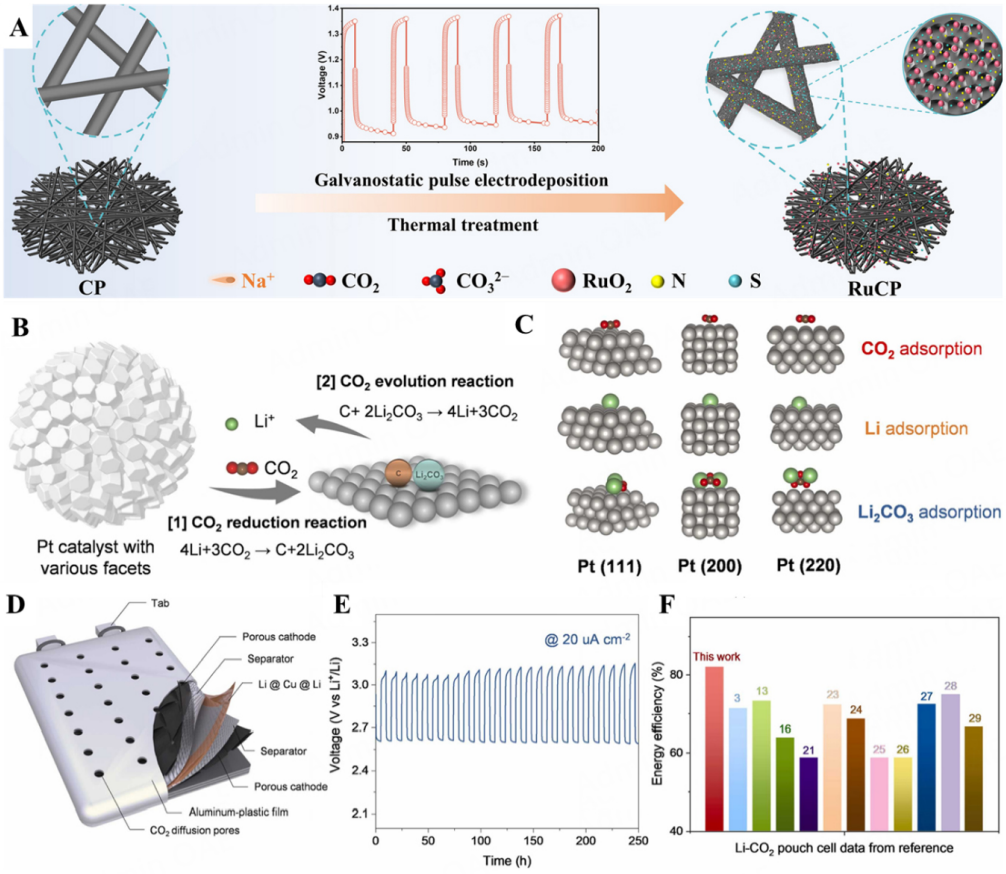

Figure 5. (A) Fabrication of RuCP[98]. (B) CO_2 conversion in Pt-based Li-CO_2 batteries. (C) Adsorption behavior of CO_2, Li and Li_2CO_3 on different orientations of Pt surface[99]. (D) Stacked Li-CO_2 pouch cell structure. (E) Cycling performance. (F) Energy efficiency comparison with other work[99]. These figures are reproduced with permission from John Wiley & Sons Australia[98] and Elsevier[99], respectively.

catalyst achieved a low overpotential (0.54 V) and stable cycling over 142 cycles, outperforming FeNC and NC catalysts. The synergy between FeNC supports and Pt active sites constrained Li_2CO_3 particle size, reducing decomposition potential and enhancing performance[103].

Iridium (Ir) and its oxides have shown excellent catalytic performance in CO_2RR, reducing overpotentials, increasing discharge capacity, and influencing discharge product formation. For example, Xing *et al.* synthesized ultrathin Ir nanosheets supported on N-doped carbon nanofibers (Ir NSs-CNFs), which stabilized intermediate products such as $Li_2C_2O_4$ during discharge[104]. This stabilization delayed the formation of plate-like Li_2CO_3, enabling easier decomposition of discharge products at lower charging voltages and improving the cycling performance of Li-CO_2 batteries. IrO_2, in particular, is highly stable and active in oxygen evolution and CO_2-related reactions. IrO_2/carbon fibers derived from kapok (IrO_2/CK) were developed using simple carbonization and hydrothermal processes[105]. These cathodes demonstrated excellent CO_2 catalytic activity, enhanced electron transfer, and efficient space for Li_2CO_3 deposition, enabling Li-CO_2 batteries to operate for over 4,000 h. Another example is NCNTs modified with ultrafine IrO_2 nanoparticles (IrO_2-N/CNT)[106]. Batteries using these cathodes achieved high capacities (4,634 mAh g^{-1}), low overpotentials (3.95/1.34 V), and extended cycling lives (over 2,500 h or 316 cycles). These studies highlight the potential of IrO_2 as a key material for advancing efficient and long-lasting Li-CO_2 batteries. Beyond Ir, noble metals such as Pd have shown promise, with Pd-coated nanoporous gold

(NPG@Pd) cathodes for Al-CO_2 batteries achieving high energy efficiency (up to 87.7%) and small discharge-charge voltage gaps (as low as 0.091 V)[107]. Similarly, PdO has shown potential in enhancing CO_2 reduction efficiencies, particularly in hybrid or composite configurations[108].

Non-noble metal/carbon composites

Non-noble metals such as Ni, Co, Mo, Cu, Fe, and Mn, along with their composites, are among the most promising catalysts due to their abundance, cost-effectiveness, environmental benefits, and, importantly, their tunable structures and multivalence states. These metals can form a wide variety of oxides, sulfides, nitrides, and phosphides with distinct crystal structures, leading to excellent electrochemical catalytic performance. Numerous nanomaterials, including nanoparticles, nanosheets, and nanorods, have been developed for catalysts such as MoS_2, Mo_2C, WSe_2, and VS_2, all of which demonstrate high catalytic activity[109,110].

A major challenge in using MoS_2 as a CO_2RR catalyst is its highest catalytic activity being confined to edge sites, coupled with limited electron transfer due to its semiconducting nature. To address this, heterostructures generating localized electric fields can enhance intermediate interactions and overall performance. Naik *et al.* developed a $NiFe_2O_4$/MoS_2/MWCNTs heterostructure using a two-step hydrothermal process for Li-CO_2 batteries under simulated Martian conditions[111]. $NiFe_2O_4$, a p-type inverse spinel oxide, forms heterojunctions with MoS_2, modifying its electronic properties and enhancing CO_2RR through interfacial interactions. MWCNTs ensure efficient electron flow, reducing charge transfer resistance. This cathode achieved a high discharge capacity of 26,533.5 mAh g^{-1} with strong cycling stability, demonstrating its potential for high-performance M-CO_2 batteries, as shown in Figure 6A and B[111]. Peng *et al.* synthesized Cu_3P/C nanocomposites through phosphatization of a copper-based MOF precursor for use in Zn-CO_2 batteries, achieving a strong performance with an open-circuit voltage of 1.5 V[112].

Transition metal catalysts coordinated with nitrogen on carbon supports, particularly those involving Fe, Co, Ni, Cu, and Bi, have shown great promise for CO_2 reduction in M-CO_2 batteries. For example, ultrathin Cu-N_2/GN nanosheets achieved a peak power density of 0.6 mW cm^{-2} in Zn-CO_2 batteries, while Fe_1NC/S_1-1000 catalysts with atomic Fe-N_3 sites reached 0.5 mW cm^{-2}[113]. However, low power densities, with CO as the primary CO_2RR product, remain a challenge. To address this, Bi clusters (BiC/HCS) on hollow carbon spheres achieved a peak power density of 7.2 mW cm^{-2}, exceeding 200 recharge cycles and demonstrating 68.9% energy efficiency for formate production, paving the way for practical advancements[110]. Carbon-based transition metal oxides and sulfides in composite materials offer excellent catalytic properties, making them ideal for M-CO_2 battery applications. Liu *et al.* demonstrated the pivotal role of octahedral Co sites in Co_3O_4, where low eg orbital filling enhanced CO_2-catalyst bonding, leading to a low overpotential of 1.0 V and a 600-h cycle life for Li-CO_2 batteries[114]. Co/Co_9S_8 nanoparticles anchored on S, N co-doped porous carbon (Co/Co_9S_8@SNHC) exhibited superior catalytic activity in Na-CO_2 batteries, achieving an areal capacity of 18.9 mAh cm^{-2} at 0.5 mA cm^{-2}[115]. Xu *et al.* developed Fe-Cu-N-C catalysts with synergistic Fe/Fe_3C nanocrystals, Fe-N_x, and Cu-N_x sites, achieving a low voltage gap of 0.44 V and over 1,550 cycles, showcasing excellent durability and performance[75].

Manganese-based catalysts excel in CO_2RR and CO_2ER due to their diverse crystal structures, valence states, and electronic configurations[116-118]. Liu *et al.* developed a 3D nanofiber framework with dual Mn active sites (MOC) supported on N-doped carbon nanofibers (MOC@NCNF) via electrospinning[119]. They observed *in situ* electrochemical reconstruction between Mn(II) and Mn(III) during cycling [Figure 6C]. During charging, Mn(II) oxidizes to Mn(III), generating abundant Mn(III) active sites, which revert to Mn(II) during discharge. DFT calculations revealed that Mn(II) lowers energy barriers for CO_2RR intermediates,

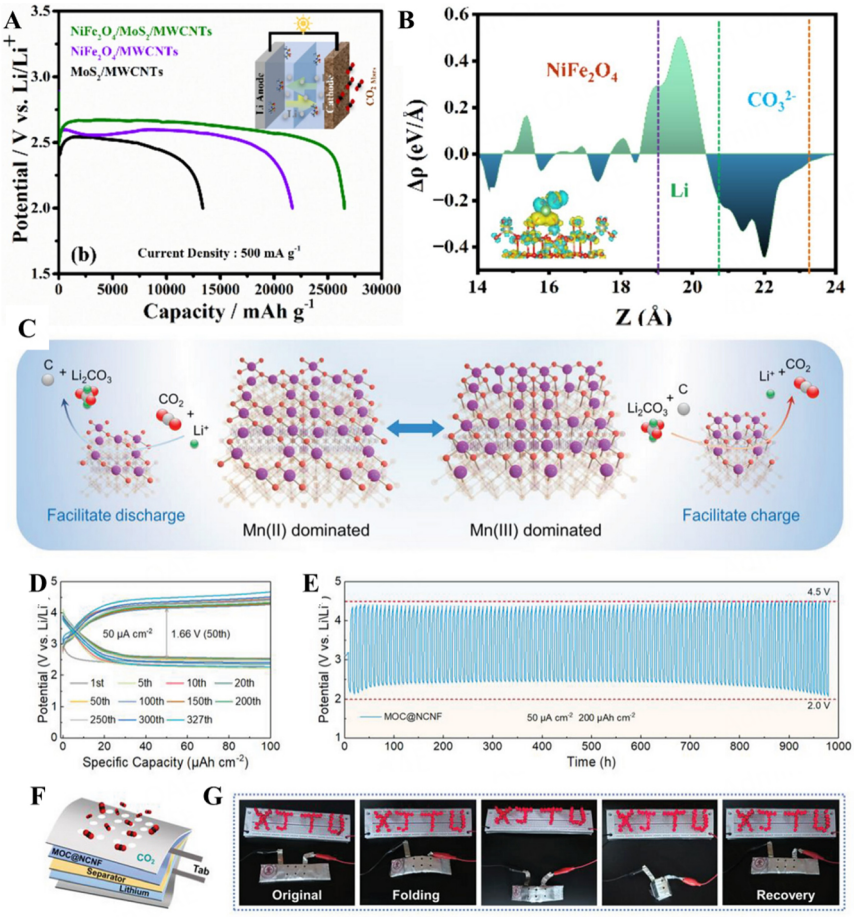

Figure 6. (A) Discharge profiles for Li-$CO_{2\ Mars}$ batteries. (B) 1-D charge density profile for Li_2CO_3 adsorption on the $NiFe_2O_4/MoS_2$[111]. (C) MOC@NCNF electrochemical reconstruction mechanisms. (D) Discharge and charge profiles, and (E) Cycle performance of MOC@NCNF. (F) Schematic of flexible Li-CO_2 battery. (G) LEDs powered by flexible Li-CO_2 batteries at various bending states[119]. These figures are reproduced with permission from Elsevier[111] and Wiley[119], respectively.

while Mn(III) activates $Li_2C_2O_4$ during CO_2ER, facilitating Li-O bond cleavage. Li-CO_2 batteries with MOC@NCNF cathodes achieved high discharge capacity (10.31 mAh cm^{-2}), energy efficiency (64.94%), and prolonged cycle life (327 cycles, 1,308 h) at 50 μA cm^{-2} [Figure 6D and E]. The flexible MOC@NCNF electrode also supports wearable electronics, maintaining performance under bending and folding [Figure 6F and G].

Single-atom catalysts

SACs, particularly metal-NC catalysts with single metal atoms such as Cu, Ni, Fe, Ru, and Co, have gained significant attention due to their high atomic utilization and strong interfacial electronic interactions[120-123]. Theoretically, the metal dispersion in SACs approaches 100%, with unique metal coordination environments providing maximum atomic efficiency and distinct catalytic properties[18,124-126].

Well-defined and uniformly dispersed structures offer significant potential for enhancing catalytic activity and selectivity in M-CO_2 batteries. Rho *et al.* demonstrated that noble metal catalysts, such as Ru and Ir, achieve lower overpotentials at the single-atom scale, highlighting improved catalytic efficiency with reduced particle size[100]. Miao *et al.* developed a Ni-N_4-SAC catalyst by annealing nickel nitrate and polyacrylonitrile (PAN) within a zeolitic framework, achieving Ni clusters (0.5 and 0.8 nm) alongside Ni-N_4

sites[123]. Synergistic interactions between Ni clusters and Ni-N_4 sites enhanced CO_2 activation, as shown in Figure 7A and B, achieving a peak power density of 11.7 mW cm^{-2} in Zn-CO_2 batteries with stability over 1,200 cycles[123]. A Cu-N_4 SAC (Cu/NCNF) for Li-CO_2 batteries was synthesized, which demonstrated high capacity (14,084 mAh g^{-1}), low polarization (1.29 V), and 133-cycle stability[127]. The Cu-N_4 centers promoted CO_2 adsorption and discharge product decomposition, highlighting the impact of SACs on efficiency and durability.

The coordination environment of metal SAs (SACs) offers enhanced design flexibility compared to nanoparticles, enabling superior catalytic performance. For example, Zhu *et al.* developed a Cd-N_4 SAC (Cd SAs/NC) anchored on N-doped carbon by impregnating carbon black with cadmium nitrate and PAN, followed by calcination at 500-700 °C [Figure 7C][128]. X-ray absorption fine structure (XAFS) analysis confirmed atomic dispersion, with Cd in the +2 oxidation state and a Cd-N bond length of 2.24 Å [Figure 7D and E]. Cd SAs/NC-600 demonstrated outstanding CO_2RR and CO_2ER performance, achieving a record-high discharge capacity of 160,045 mAh g^{-1} at 500 mA g^{-1}, ultra-low overpotential of 1.74 V at 2 A g^{-1}, and stable performance over 1,680 cycles, as depicted in Figure 7F and G. DFT calculations revealed the atomic dispersion of Cd coordinated with four pyridinic nitrogen atoms, contributing to the catalyst's high activity[128]. Li *et al.* optimized Pd-SACs by anchoring Pd_1-O_3C_1 sites on oxidized mesoporous carbon (Pd_1-O-CB)[129]. This design led to excellent CO selectivity (98.7% at 0.47 V) and high current density (280.4 mA cm^{-2}) Pd_1-O-CB demonstrated over 48 h of stability and a peak power density of 1.72 mW cm^{-2} in a Zn-CO_2 battery.

SACs offer unique advantages, including maximized metal utilization, tunable catalytic sites, and cost-effectiveness, making them highly promising for M-CO_2 battery applications. However, challenges such as particle aggregation, dissolution, and the optimization of SAC loading on carbon carriers must be addressed. Future research should focus on enhancing SAC stability, preventing aggregation through advanced carrier designs, and elucidating the relationship between SAC loading and battery performance to unlock their full potential.

Metal-organic frameworks

MOFs, with tunable functionality and structural versatility, are widely studied for CO_2 capture, separation, and catalytic conversion. Tailored pore sizes and functional groups enhance CO_2 adsorption, while MOF nanostructures support uniform Li_2CO_3 nucleation and deposition[130]. Li *et al.* studied various MOFs, with Mn_2(dobdc) achieving a discharge capacity of 18,022 mAh g^{-1} at 50 mA g^{-1}, while Mn(HCOO)$_2$ maintaining a stable ~4 V charge potential at 200 mA g^{-1}[131]. Additionally, ultrafine MnO nanoparticles in a N-doped carbon framework (MnO@NC-G) enabled fast electron transfer and rapid mass diffusion, achieving 25,021 mAh g^{-1} at 50 mA g^{-1} with stable cycling over 10 cycles[132]. Mn(II)-based MOFs demonstrate high porosity, low charge potential, and excellent performance, even at high current densities.

In conventional Li-CO_2 systems, $Li_2C_2O_4$ disproportionates into Li_2CO_3, causing energy loss and voltage drops. Recent advancements using solid redox mediators (RMs), such as a Cu(II)-based MOF with benzene-1,3,5-tricarboxylate (BTC), address this issue [Figure 8A and B][133]. With a high surface area (1,650 m^2 g^{-1}) and 9 Å pore size, the MOF enhances CO_2 adsorption and catalytic activity. Paired with CNTs, the RM-based cathode achieves 3 S cm^{-1} conductivity, reducing polarization and stabilizing $Li_2C_2O_4$. This increases discharge voltage (2.8 V), lowers charge voltage (3.7 V), and enables stable cycling for over 400 cycles [Figure 8C and D]. DFT calculations confirm RM(II)-BTC's strong adsorption of $Li_2C_2O_4$, preventing its disproportionation to Li_2CO_3.

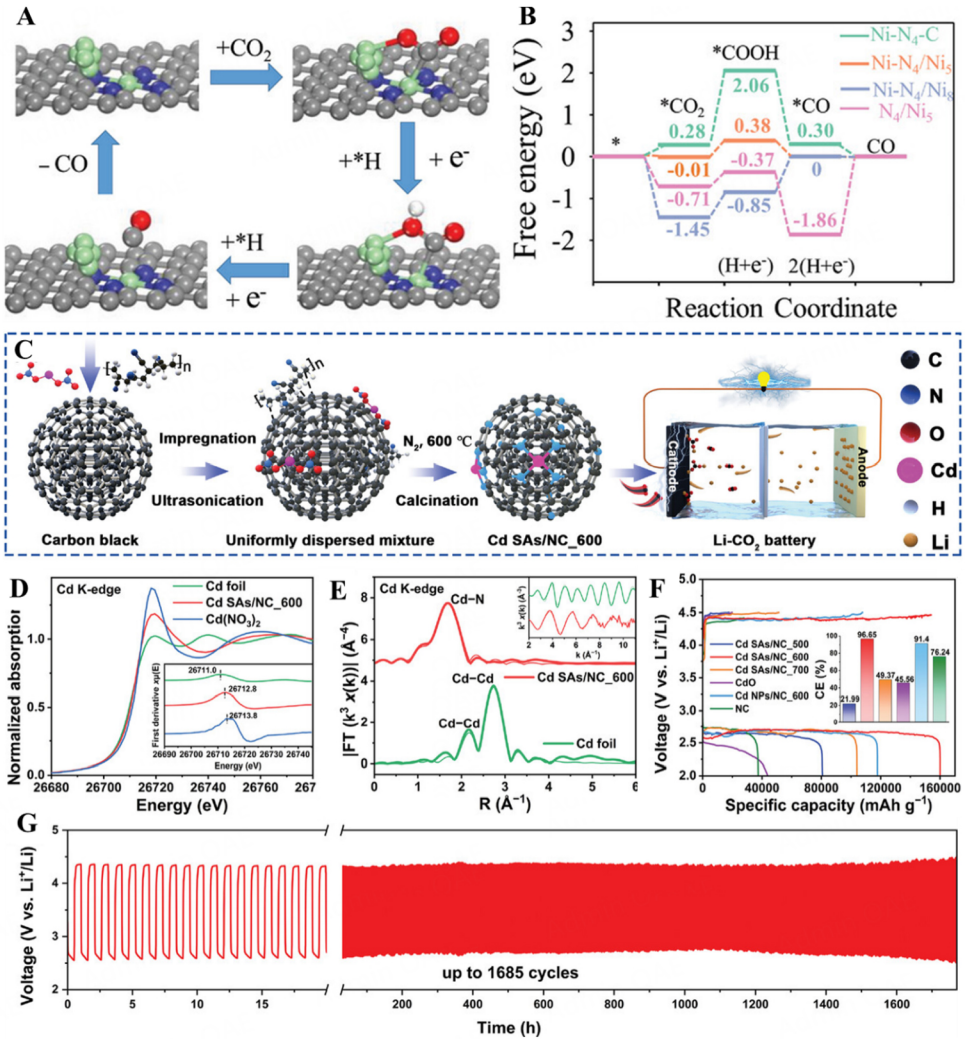

Figure 7. (A) Proposed CO_2RR pathways using Ni-N_4/Ni_5. (B) Free-energy diagram of CO_2RR to CO[123]. (C) Preparation of Cd SAs/NC. (D) Cd K-edge XANES spectra and first derivatives (inset) of Cd foil, Cd SAs/NC-600, and $Cd(NO_3)_2$. (E) Cd K-edge EXAFS spectra in the R-space and k-space (inset) of Cd foil and Cd SAs/NC-600. (F) Full charge-discharge profiles. (G) Cycling performance of Cd SAs/NC-600[128]. These figures are reproduced with permission from Wiley[123,128].

Covalent organic frameworks (COFs), similar to MOFs, are crystalline porous materials with large surface areas, tunable structures, and ease of functionalization[134,135]. Their thermal and chemical stability makes them ideal for gas storage, adsorption, and catalysis[136]. Metalloporphyrin-based COFs enhance CO_2 capture, mass transfer, and ion migration, enabling precise CO_2RR critical for electrocatalysis[136]. For example, hydrazine-linked COFs [e.g., benzene-1,3,5-tricarboxaldehyde (Tf)-2,5-dipropoxyterephthalohydrazide (DHzOPr)] improve CO_2 adsorption and Li^+ migration at Ru/CNT cathodes, boosting Li-CO_2 battery performance[137]. Zhang *et al.* developed TTCOF-Mn, a porphyrin-based COF catalyst featuring Mn(II) porphyrin sites, uniform microporous channels, and abundant catalytic sites [Figure 8E-G][138]. TTCOF-Mn achieved a low potential gap (1.07 V at 100 mA g^{-1}) and stable cycling for 180 cycles at 300 mA g^{-1}. Simulations revealed superior CO_2 adsorption (-0.02 eV free energy) and efficient four-electron CO_2 conversion of Mn-TAPP sites, corroborated by DFT analysis.

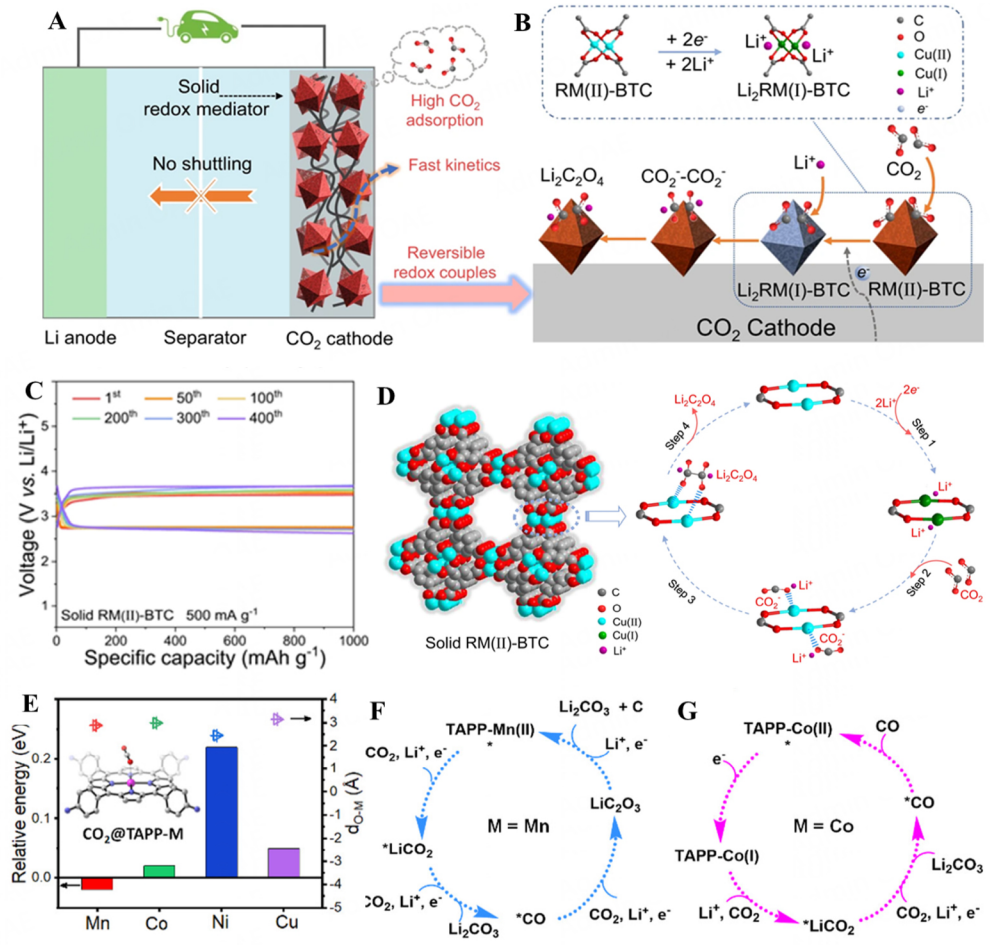

Figure 8. (A) Schematic of a Li-CO_2 battery with a solid RM(II)-BTC. (B) RM(II)-BTC reaction mechanism, showing reduction, CO_2 reaction, and $Li_2C_2O_4$ formation. (C) Cycling performance. (D) 3D space-filling diagram and reaction schematic for $Li_2C_2O_4$ formation[133]. (E) DFT-calculation energy profiles of CO_2 adsorption on TAPP-M (M = Mn, Co, Ni, Cu) molecules. (F) Four-electron pathway at the TAPP-Mn site. (G) Two-electron pathway at the TAPP-Co site[138]. These figures are reproduced with permission from Nature Publishing Group[133] and American Chemical Society[138], respectively.

Crystalline organic frameworks, including MOFs, COFs, and hydrogen-bonded organic frameworks (HOFs)[139], feature multifunctional porous networks. HOFs, self-assembled via hydrogen bonding, are cost-effective but often lack structural stability[140-142]. Strategies such as π-π stacking and double hydrogen bonds have improved HOF stability, enabling their use in Li-CO_2 batteries[143-146]. Cheng *et al.* developed a high-performance HOF-based cathode by combining ultra-stable HOF-FJU-1 with Ru@CNT[147]. HOF-FJU-1, synthesized from 3,3′,6,6′-tetracyano-9,9′-bicarbazole, features π-π interactions, as shown in Figure 9A and B, and high resistance to solvents, temperature, and acids/bases. This cathode delivers high capacity (24,245 mAh g^{-1} at 100 mA g^{-1}), ultralow overpotential (1.09 V), and stable cycling over 1,800 h at 400 mA g^{-1}, even at 5 A g^{-1}, demonstrating excellent stability and promising applications for high-rate, durable Li-CO_2 batteries [Figure 9C and D].

MOFs, COFs, and HOFs exhibit unique advantages in M-CO_2 batteries due to their high tunability, large surface area, and diverse functional sites. These properties enhance CO_2 adsorption, facilitate efficient CO_2RR and CO_2ER, and support the uniform distribution of discharge products. MOFs, in particular, have demonstrated excellent electrochemical performance in terms of capacity, discharge voltage, and stability

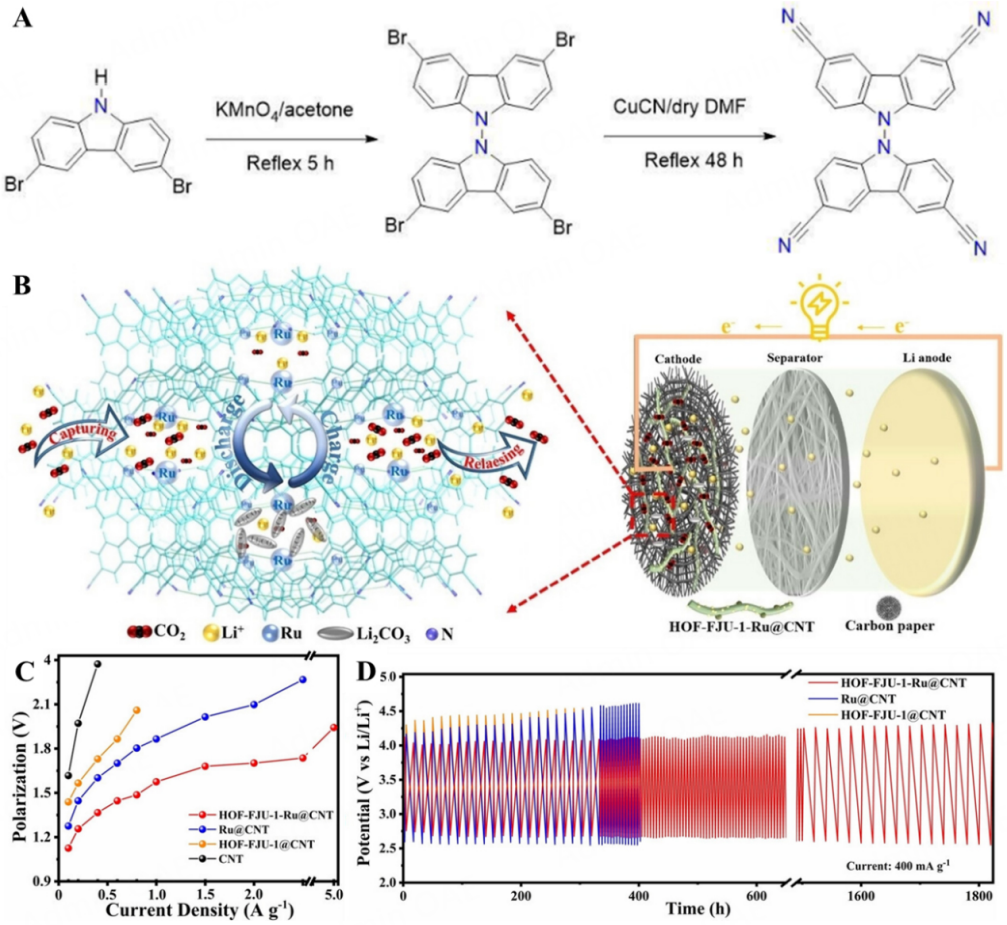

Figure 9. (A) Schematic of tetracyano-bicarbazole monomer synthesis. (B) Diagram of a Li-CO_2 battery. (C) Overpotentials at different current densities. (D) Battery lifespan at 400 mA g^{-1}[147]. This figure is reproduced with permission from Wiley[147].

when combined with materials such as Ru nanoparticles or CNTs. However, the long-term stability of MOFs, especially HOFs, under extreme electrochemical conditions remains a significant challenge. Future research should focus on improving the stability of these materials, particularly by hybridizing them with stable, conductive supports and exploring novel structural modifications to enhance their robustness. Furthermore, further investigation into optimizing pore size and improving the interaction between metal centers and CO_2 intermediates will be crucial to advancing MOF-based cathodes for high-performance, durable M-CO_2 batteries.

Other carbon materials (self-supporting cathodes)

Conventional M-CO_2 batteries face limitations due to powder-based electrodes requiring polymer binders and rigid 2D current collectors, which reduce flexibility, conductivity, and cycle stability, making them unsuitable for wearable devices[74,115,148,149]. Additionally, traditional carbon nanomaterials often show limited catalytic activity. Freestanding electrodes address these issues by eliminating binders and rigid collectors, offering flexibility, uniform catalyst distribution, efficient electron transport, and reduced material agglomeration. These properties enhance catalytic activity, stability, and electrochemical performance, making them ideal for wearable energy storage. For instance, Xiao *et al.* developed a binder-free, freestanding N-doped 3D CNT/graphene cathode, achieving high specific capacity (17,534.1 mAh g^{-1}), low overpotential (1.13 V), and excellent cycle stability over 180 cycles[150].

Developing flexible, lightweight, and robust fibrous cathodes with high catalyst loading, efficient electron transport, and strong catalyst-current collector bonding is a critical challenge[151]. Traditional methods often suffer from poor catalyst dispersion and weak interfacial bonding due to binder reliance, limiting performance and durability[152]. Chen *et al.* addressed this by designing a flexible, stretchable, waterproof, and fireproof fiber-shaped Li-CO_2 battery with a "spring-like" architecture[153]. The carbon fiber hybrid bundle (CFB)@NCNT-Mo_2N cathode was fabricated via chemical vapor deposition (CVD) of porous NCNTs on carbon fibers, followed by atomic layer deposition (ALD) of Mo_2N. Combined with a gel polymer electrolyte (GPE) and a CNT-based anode, the design achieved 14,250 Wh kg^{-1} energy density, a 0.87 V voltage gap, and 525-cycle stability. This battery maintained performance under extreme conditions, offering a promising solution for wearable Li-CO_2 batteries in challenging environments. Investigating four-electron reaction pathways in Li-CO_2 batteries is crucial due to the slow kinetics of Li_2CO_3 formation. Hu *et al.* developed a binder-free, self-supporting Mo_2C nanowire (Mo_2C-NWs) electrode to enhance the four-electron $Li_2C_2O_4$ pathway[154]. This design significantly improved cycle life, rate performance, and capacity. *In-situ* Fourier transform infrared (FTIR) spectroscopy confirmed the formation of $Li_2C_2O_4$ and Li_2CO_3 at varying discharge depths [Figure 10A] revealing a mechanism to regulate product formation on the Mo_2C cathode. Electrochemical testing showed the Mo_2C-NWs cathode achieved an ultra-low overpotential of 0.35 V, significantly outperforming CNT (2.60 V) cathodes [Figure 10B]. Additionally, the lower charge potential of the Mo_2C cathode (3.31 V) minimized overpotentials, improving cycle life and battery efficiency. The Mo_2C-NWs-based battery demonstrated exceptional performance, surpassing 165 cycles at 0.1 mA cm^{-2} [Figure 10C]. As portable energy storage devices evolve, the high performance of liquid batteries has inspired the development of flexible batteries. A flexible Li-CO_2 battery was created using an integrated CNT/MoO_3 composite, eliminating the need for binders or metal current collectors[155]. This battery demonstrated a high discharge capacity of 121.06 mAh cm^{-2}, a low charge voltage under 3.8 V, and 300 cycles at 0.25 mA cm^{-2}, maintaining stable performance under bending and twisting. Additionally, a Mo_2N-ZrO_2@NCNF bifunctional heterostructure catalyst was developed, enhancing CO_2 conversion and reversible $Li_2C_2O_4$ formation[156]. The synthesis involves reacting $ZrCl_4$ with two organic ligands in a N,N-dimethylformamide (DMF)/H_2O mixture to form D-UiO-66-NH_2 [Figure 10D]. This design improves cycling stability and energy efficiency, offering a promising strategy for advanced energy storage devices.

The positive electrode of a Li-CO_2 battery typically consists of a mixed electrocatalyst, conductive carbon material, an organic binder, and a current collector[157,158]. Traditional preparation methods are time- and energy-intensive, and the inclusion of insulating binders can increase internal resistance, thereby diminishing the performance of M-CO_2 batteries[3,159]. In contrast, a binder-free, self-supporting cathode catalyst enhances electrode performance by integrating high electrochemical efficiency and stretchability[153,160]. This design supports the development of advanced energy storage systems for high-performance, multifunctional wearable electronic devices.

CONCLUSION AND FUTURE PROSPECT

This review provides a comprehensive examination of the applications of various carbon-based materials and their enhancement strategies in M-CO_2 batteries. It emphasizes the intricate relationships between carbon material structure, composition, and electrochemical performance. Key findings are systematically summarized in Table 1, which includes detailed comparisons of battery types, operating atmospheres, cathode materials, electrolytes, voltage gaps (with applied current), discharge capacities (relative to current density), and cyclability (cycle life, cut-off conditions, and current density). This detailed analysis offers valuable insights into optimizing carbon-based materials for enhanced battery performance and durability. However, there are still technical challenges such as insufficient electrocatalytic activity, insufficient catalyst stability/durability, insufficient catalyst design, selection and performance optimization strategies, and

Table 1. A performance comparison of carbon-based cathode material for different Metal-CO_2 batteries

Battery type	Atmosphere	Cathode materials	Electrolyte	Voltage gap, applied current	Discharge capacity/current density	Cyclability (cycle life/cut-off condition/current density)	Ref.
Li-CO_2	Pure CO_2	Conductive carbon	1 M LiTFSI/[bmim]Tf_2N	-	2,500 mAh g^{-1}	-	[161]
Li-CO_2	Pure CO_2	CNT	1 M LiTFSI/TEGDME	-	1,000 mAh g^{-1} 150 mA g^{-1}	-	[61]
Li-CO_2	Pure CO_2	TDG	1 M LiTFSI/DMSO-0.3 M $LiNO_3$	1.87 V 2 A g^{-1}	69,000 mAh g^{-1} 500 mA g^{-1}	600 cycles with a cut-off capacity of 500 mAh g^{-1} at 1 A g^{-1}	[67]
Li-CO_2	Pure CO_2	Porous Pt@carbon cloth	1 M LiTFSI/TEGDME	0.45 V 20 μA cm^{-2}	5.81 mAh cm^{-2} 20 μA cm-$^{-2}$	Over 200 cycles at 40 μA cm^{-2}	[99]
Li-CO_2	Pure CO_2	MOC@NCNF	-	1.45 V 20 μA cm^{-2}	10.31 mAh cm^{-2} 20 μA cm^{-2}	Over 327 cycles with a fixed capacity of 100 μAh cm^{-2} at 50 μA cm^{-2}	[119]
Li-CO_2	Simulated martian atmosphere	$NiFe_2O_4/MoS_2$ /MWCNTs	1 M LiTFSI/DMSO-0.3 M $LiNO_3$	1.72 V 500 mA g^{-1}	26,533.5 mAh g^{-1} 500 mA g^{-1}	Over 195 cycles with a cut-off capacity of 500 mAh g^{-1} at 500 mA g^{-1}	[111]
Li-CO_2	Pure CO_2	Cd SAs/NC	1.2 M LiTFSI/DMSO-0.3 M $LiNO_3$	1.31 V 200 mA g^{-1}	160,045 mAh g^{-1} 500 mA g^{-1}	1,685 cycles with a capacity of 500 mAh g^{-1} at 1 A g^{-1}	[162]
Li-CO_2	Pure CO_2	Solid RM(II)-BTC/CNTs	1 M LiTFSI/TEGDME	0.9 V 100 mA g^{-1}	9,040 mAh g^{-1} 100 mA g^{-1}	400 cycles with a curtailing capacity of 1,000 mAh g^{-1} at 500 mA g^{-1}	[133]
Li-CO_2	Pure CO_2	TTCOF-Mn	1 M LiTFSI/TEGDME	1.07 V 100 mA g^{-1}	13,018 mAh g^{-1} 100 mA g^{-1}	180 cycles with a fixed capacity of 1,000 mAh g^{-1} at 300 mA g^{-1}	[138]
Li-CO_2	Pure CO_2	HOF-FJU-1-Ru@CNT	1 M LiTFSI/TEGDME	1.09 V 100 mA g^{-1}	24,245.3 mAh g^{-1} 100 mA g^{-1}	350 cycles with a capacity of 1,000 mAh g^{-1} at 400 mA g^{-1}	[147]
Li-CO_2	Pure CO_2	Mo_2C-NWs	-	0.35 V 0.05 mA cm^{-2}	8.47 mAh cm^{-2} 0.1 mA cm^{-2}	165 cycles with a limited capacity of 0.5 mAh cm^{-2} at 0.1 mA cm^{-2}	[154]
Li-CO_2	Pure CO_2	Mo_2N-ZrO_2@NCNF	1 M LiTFSI/TEGME	0.32 V 10 μA cm^{-2}	5,262.2 μAh cm^{-2} 20 μA cm^{-2}	165 cycles with a limited capacity of 0.5 mAh cm^{-2} at 50 μA cm^{-2}	[156]
Na-CO_2	Pure CO_2	Ru@CNT	1 M NaTFSI/TEGDME	1.5 V 100 mA g^{-1}	20,277 mAh g^{-1} 100 mA g^{-1}	100 cycles with a limited capacity of 500 mAh g^{-1} at 100 mA g^{-1}	[95]
Na-CO_2	Pure CO_2	a-MCNTs	PVDF-HFP-4% SiO_2/$NaClO_4$-TEGDME	0.74 V 100 mA g^{-1}	5,000 mAh g^{-1} 50 mA g^{-1}	400 cycles with a capacity of 1,000 mAh g^{-1} at 500 mA g^{-1}	[163]
Na-CO_2	CO_2/O_2	Porous carbon	1 M NaTFSI/SiO_2-IL-TFSI/PC	2.4 V 200 mA g^{-1}	800 mAh g_{carbon}^{-1} 200 mA g^{-1}	20 cycles with a cut-off capacity of 800 mAh g_{carbon}^{-1} at 200 mA mA g^{-1}	[164]
Na-CO_2	Pure CO_2	NS-PC/CP	1 M $NaClO_4$/TEGDME	1.04 V 10 uA cm^{-2}	2,422 μAh cm^{-2} 40 μA cm^{-2}	100 cycles with energy efficiencies of ≈60%	[85]
Na-CO_2	Pure CO_2	RuCP	1 M $NaPF_6$/DIGLYME	1.8 V 100 μA cm^{-2}	2,788 μAh cm^{-2} 100 μA cm^{-2}	Over 350 cycles at 100 μA cm^{-2}	[98]
K-CO_2	Pure CO_2	B-NCNTs	1.0 M KTFSI/TEGDME	0.81 V at 50 mA g^{-1}	9,436 mAh g^{-1} at 200 mA g^{-1}	450 cycles or 3,100 h with a curtailing capacity of 500 mAh g^{-1}	[77]

K-CO_2	Pure CO_2	N-CNT/RGO 3D network	1.0 M KTFSI TEGDME	-	-	250 cycles or 1,500 h with a cut-off capacity of 300 mA h g^{-1}	[165]
Al-CO_2	Pure CO_2	NPG@PD	$AlCl_3$/[EMIm]Cl (M:M=1:3)	0.091 V 333 mA g^{-1}	-	Over 30 cycles at 333 mA g^{-1}	[107]
Al-CO_2	CO_2/O_2	Ketjenblack	[EMIm]Cl/$AlCl_3$ (M:M=1:2)	1.4 V 70 mA g_{Carbon}^{-1}	13,000 mAh g_{Carbon}^{-1} 70 mA g_{Carbon}^{-1}	50 cycles with a capacity of 200 mAh g_{Carbon}^{-1} at 70 mA g_{Carbon}^{-1}	[166]
Zn-CO_2	Pure CO_2	C-BN@600	0.1 M $KHCO_3$	0.78 V 1 mA cm^{-2}	5.42 mW cm^{-2} 39.4 mA cm^{-2}	Over 800 cycles at 1 mA cm^{-2}	[88]
Zn-CO_2	Pure CO_2	Ni-N_4/Ni_5	1 M KOH	0.393 V 50 mA cm^{-2}	-	425 h at 5 mA cm^{-2}	[123]

insufficient basic understanding of the catalyst mechanism of action in the development of practically usable M-CO_2 batteries. To address the challenges faced by carbon-based catalysts and their use as hosts for metal catalysts in M-CO_2 batteries, future research can focus on the following aspects:

(1) Enhancing electrocatalytic activity: developing carbon-based catalysts with high-density active sites through heteroatom doping, defect engineering, and edge structure modifications can significantly enhance activity. Multifunctional active sites, such as bimetallic or metal-nonmetal combinations, can improve reaction efficiency by enabling synergistic effects. Precise structural control using advanced synthesis techniques, such as tailoring hierarchical designs in graphene or CNTs, can further optimize performance.

(2) Improving catalyst stability and durability: stability can be enhanced by designing robust carbon frameworks with high corrosion resistance and strong metal-support interactions. Protective coatings or interface engineering can prevent metal nanoparticle detachment or agglomeration during operation. Additionally, understanding degradation mechanisms, such as poisoning and structural collapse under long-term use, will allow for the development of more durable catalysts.

(3) Catalyst design and optimization strategies: leveraging computational methods and machine learning enables the rapid prediction of optimal catalyst compositions and configurations. Tailoring metal-carbon interfaces to enhance electron transfer and catalytic synergy is critical. Multi-scale porous structures can improve reactant mass transfer and active site accessibility, leading to higher catalytic efficiency and product selectivity.

(4) Deepening understanding of catalytic mechanisms: advanced *in situ* characterization techniques, such as X-ray absorption spectroscopy and infrared spectroelectrochemistry, allow real-time monitoring of active site evolution and reaction pathways. Identifying intermediates and activation barriers will clarify reaction mechanisms. Integration of theoretical and experimental approaches can guide the rational design of next-generation catalysts.

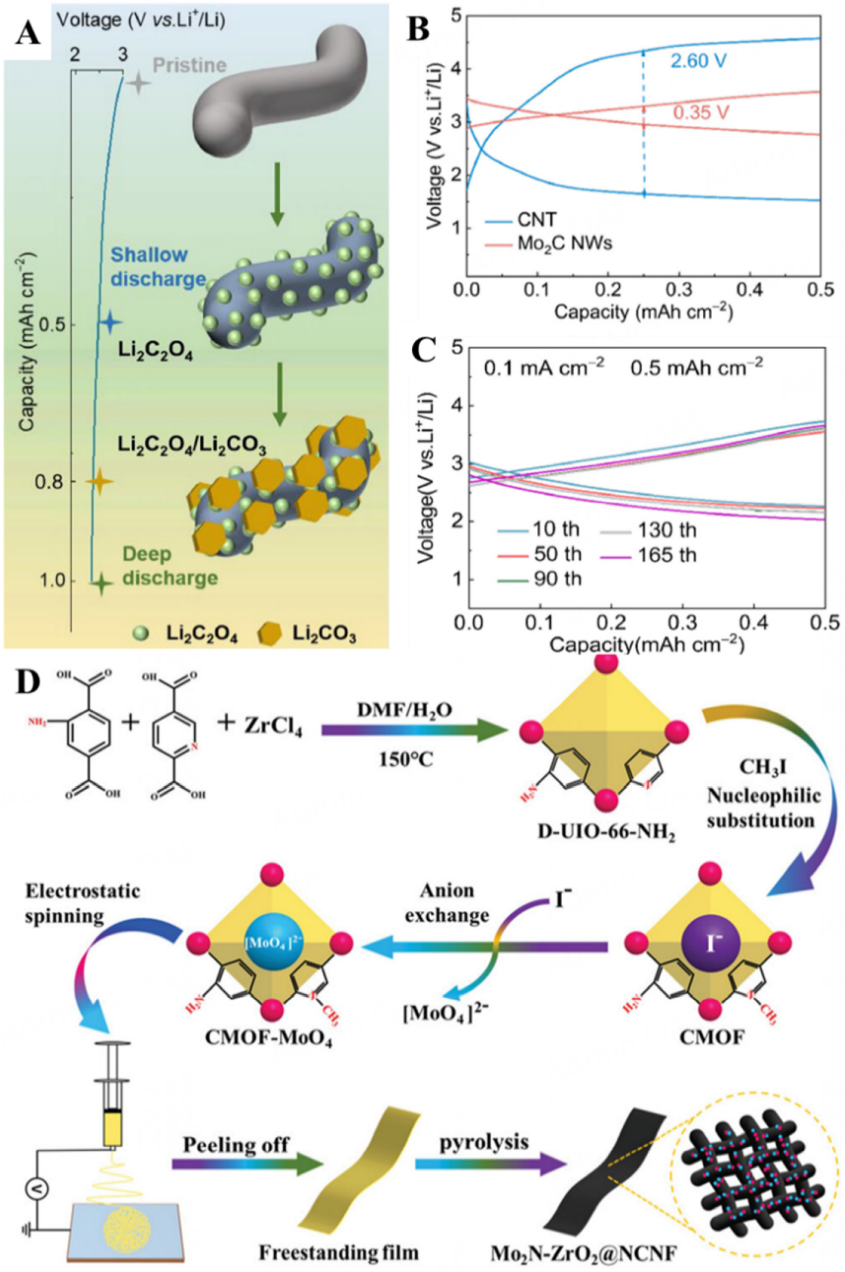

Figure 10. (A) Schematic of the discharge products in the Mo_2C-NWs cathode. (B) First cycle discharge/Charge curves of Li-CO_2 battery with CNT and Mo_2C-NWs electrodes. (C) Cycling performance of the Mo_2C-NWs electrode under CO_2[154]. (D) Schematic of Mo_2N-ZrO_2@NCNF synthesis[156]. These figures are reproduced with permission from Elsevier[154] and Wiley[156], respectively.

(5) Development of green and sustainable catalysts: replacing precious metals with earth-abundant alternatives, such as iron, cobalt, and nickel, can reduce costs. Biomass-derived carbon materials, as catalyst supports, enhance sustainability. Designing recyclable and regenerable catalysts with stable performance over multiple cycles is crucial for environmental and economic feasibility in large-scale applications.

DECLARATIONS

Acknowledgments

The authors acknowledge support from the German Research Foundation and the Sino-German Centre for Research Promotion. Dong, Y. appreciates the support from the Postdoctoral scholarship for women scientists. Xu, C. and Fu, Y. appreciate the support from the China Scholarship Council.

Authors' contributions

Conceived and wrote the manuscript: Dong, Y.; Xu, C.
Reviewed the manuscript: Dong, Y.; Xu, C.; Lei, Y.
Contributed to the discussion of the manuscript: Dong, Y.; Xu, C.; Fu, Y.; Zhao, H.; Lei, Y.

Availability of data and materials

Not applicable.

Financial support and sponsorship

The manuscript support from the German Research Foundation (DFG, Project number 501766751), the Sino-German Centre for Research Promotion (GZ1579), start-up funding within the Postdoctoral scholarship for women scientists and the China Scholarship Council.

Conflicts of interest

All authors declared that there are no conflicts of interest.

Ethical approval and consent to participate

Not applicable.

Consent for publication

Not applicable.

REFERENCES

1. Lu, S.; Zhang, S.; Liu, Q.; et al. Recent advances in novel materials for photocatalytic carbon dioxide reduction. *Carbon. Neutralization.* **2024**, *3*, 142-68. DOI
2. Feng, D.; Li, Z.; Guo, H.; et al. Conjugated polyimides modified self-supported carbon electrodes for electrochemical conversion of CO_2 to CO. *Energy. Mater.* **2024**, *4*, 400069. DOI
3. Zheng, Z.; Wu, C.; Gu, Q.; Konstantinov, K.; Wang, J. Research progress and future perspectives on rechargeable Na-O_2 and Na-CO_2 batteries. *Energy. Environ. Mater.* **2021**, *4*, 158-77. DOI
4. Nyhus, A. H.; Yliruka, M.; Shah, N.; Chachuat, B. Green ethylene production in the UK by 2035: a techno-economic assessment. *Energy. Environ. Sci.* **2024**, *17*, 1931-49. DOI
5. Ramadhany, P.; Luong, Q.; Zhang, Z.; et al. State of play of critical mineral-based catalysts for electrochemical E-refinery to synthetic fuels. *Adv. Mater.* **2024**, *36*, e2405029. DOI
6. Fang, W.; Lu, R.; Li, F. M.; et al. Low-coordination nanocrystalline copper-based catalysts through theory-guided electrochemical restructuring for selective CO_2 reduction to ethylene. *Angew. Chem. Int. Ed.* **2024**, *63*, e202319936. DOI
7. Xu, C.; Dong, Y.; Zhao, H.; Lei, Y. CO_2 conversion toward real-world applications: electrocatalysis versus CO_2 batteries. *Adv. Funct. Mater.* **2023**, *33*, 2300926. DOI
8. Dong, Y.; Yan, C.; Zhao, H.; Lei, Y. Recent advances in 2D heterostructures as advanced electrode materials for potassium-ion batteries. *Small. Struct.* **2022**, *3*, 2100221. DOI
9. Aslam, M. K.; Wang, H.; Chen, S.; Li, Q.; Duan, J. Progress and perspectives of metal (Li, Na, Al, Zn and K)-CO_2 batteries. *Mater. Today. Energy.* **2023**, *31*, 101196. DOI
10. Zou, J.; Liang, G.; Zhang, F.; Zhang, S.; Davey, K.; Guo, Z. Revisiting the role of discharge products in Li-CO_2 batteries. *Adv. Mater.* **2023**, *35*, e2210671. DOI PubMed

11. Ampelli, C.; Tavella, F.; Giusi, D.; Ronsisvalle, A. M.; Perathoner, S.; Centi, G. Electrode and cell design for CO_2 reduction: a viewpoint. *Catal. Today.* **2023**, *421*, 114217. DOI
12. Li, X.; Zhang, K.; Li, Z.; et al. Rational design of covalent organic frameworks as gas diffusion layers for multi-atmosphere lithium-air batteries. *Angew. Chem. Int. Ed.* **2023**, *62*, e202217869. DOI
13. Wang, Z.; Sun, C.; Lu, L.; Jiao, L. Recent progress and perspectives of solid state Na-CO_2 batteries. *Batteries* **2023**, *9*, 36. DOI
14. Song, W.; Xiao, C.; Ding, J.; et al. Review of carbon support coordination environments for single metal atom electrocatalysts (SACS). *Adv. Mater.* **2024**, *36*, e2301477. DOI
15. Wang, Y.; Chu, F.; Zeng, J.; et al. Single atom catalysts for fuel cells and rechargeable batteries: principles, advances, and opportunities. *ACS. Nano.* **2021**, *15*, 210-39. DOI
16. Shah, S. S. A.; Najam, T.; Bashir, M. S.; Peng, L.; Nazir, M. A.; Javed, M. S. Single-atom catalysts for next-generation rechargeable batteries and fuel cells. *Energy. Storage. Mate.* **2022**, *45*, 301-22. DOI
17. Lin, J.; Song, W.; Xiao, C.; et al. A comprehensive overview of the electrochemical mechanisms in emerging alkali metal-carbon dioxide batteries. *Carbon. Energy.* **2023**, *5*, e313. DOI
18. Liu, W.; Cai, C.; Zhang, Z.; et al. Advancements in metal-CO_2 battery technology: a comprehensive overview. *Nano. Energy.* **2024**, *129*, 109998. DOI
19. Douka, A. I.; Yang, H.; Huang, L.; et al. Transition metal/carbon hybrids for oxygen electrocatalysis in rechargeable zinc-air batteries. *EcoMat* **2021**, *3*, e12067. DOI
20. Xu, Y.; Gong, H.; Ren, H.; et al. Highly efficient Cu-porphyrin-based metal-organic framework nanosheet as cathode for high-rate Li-CO_2 battery. *Small* **2022**, *18*, e2203917. DOI
21. Zhao, C.; Dai, X.; Yao, T.; et al. Ionic exchange of metal-organic frameworks to access single nickel sites for efficient electroreduction of CO_2. *J. Am. Chem. Soc.* **2017**, *139*, 8078-81. DOI
22. Gao, S.; Li, H.; Lu, Z.; et al. Isolated FeN_3 sites anchored hierarchical porous carbon nanoboxes for hydrazine-assisted rechargeable Zn-CO_2 batteries with ultralow charge voltage. *Carbon. Energy.* **2024**, e637. DOI
23. Yang, X.; Zhang, D.; Zhao, L.; et al. Upgrading cycling stability and capability of hybrid Na-CO_2 batteries via tailoring reaction environment for efficient conversion CO_2 to HCOOH. *Adv. Energy. Mater.* **2024**, *14*, 2304365. DOI
24. Xu, C.; Hong, P.; Dong, Y.; et al. Multiscale defective interfaces for realizing Na-CO_2 batteries with ultralong lifespan. *Adv. Mater.* **2024**, *36*, e2409533. DOI PubMed PMC
25. Xu, C.; Dong, Y.; Shen, Y.; et al. Fundamental understanding of nonaqueous and hybrid Na-CO_2 batteries: challenges and perspectives. *Small* **2023**, *19*, e2206445. DOI
26. Li, C.; Yuan, Y.; Yue, M.; et al. Recent advances in pristine iron triad metal-organic framework cathodes for alkali metal-ion batteries. *Small* **2024**, *20*, e2310373. DOI
27. Tan, C.; Wang, A.; Cao, D.; et al. Unravelling the complex Na_2CO_3 electrochemical process in rechargeable Na-CO_2 batteries. *Adv. Energy. Mater.* **2023**, *13*, 2204191. DOI
28. Liu, Y.; Mao, R.; Chen, B.; et al. Atomic design of bidirectional electrocatalysts for reversible Li-CO_2 batteries. *Mater. Today.* **2023**, *63*, 120-36. DOI
29. Chen, H.; Li, X.; Xue, H.; et al. Recent advances in the mechanism and catalyst design in the research of aprotic, photo-assisted, and solid-state Li-CO_2 batteries. *Inorg. Chem. Front.* **2024**, *11*, 5833-57. DOI
30. Xie, Z.; Zhang, X.; Zhang, Z.; Zhou, Z. Metal-CO_2 batteries on the road: CO_2 from contamination gas to energy source. *Adv. Mater.* **2017**, *29*, 1605891. DOI
31. Jaradat, A.; Ncube, M. K.; Papailias, I.; et al. Fast charge-transfer rates in Li-CO_2 batteries with a coupled cation-electron transfer process. *Adv. Energy. Mater.* **2024**, *14*, 2303467. DOI
32. Xu, C.; Fang, X.; Zhan, J.; Chen, J.; Liang, F. Progress for Metal-CO_2 batteries: mechanism and advanced materials. *Prog. Chem.* **2020**, *32*, 836. DOI
33. Xu, C.; Wang, H.; Zhan, J.; Kang, Y.; Liang, F. Engineering NH_3-induced 1D self-assembly architecture with conductive polymer for advanced hybrid Na-CO_2 batteries via morphology modulation. *J. Power. Sources.* **2022**, *520*, 230909. DOI
34. Hou, Y.; Wang, J.; Liu, L.; et al. Mo_2C/CNT: an efficient catalyst for rechargeable Li-CO_2 batteries. *Adv. Funct. Mater.* **2017**, *27*, 1700564. DOI
35. Zou, L.; Zhong, F.; Liu, J.; et al. Understanding $Li_2c_2o_4$ stabilization in reversible Li-Co_2 batteries via Li^+ solvation structure and Mo^{2+} active sites. 2024. DOI
36. Zhou, J.; Li, X.; Yang, C.; et al. A quasi-solid-state flexible fiber-shaped Li-CO_2 battery with low overpotential and high energy efficiency. *Adv. Mater.* **2019**, *31*, e1804439. DOI
37. Wang, Y.; Ji, G.; Song, L.; Wang, X.; Xu, J. A highly reversible lithium-carbon dioxide battery based on soluble oxalate. *ACS. Energy. Lett.* **2023**, *8*, 1026-34. DOI
38. Jayan, R.; Islam, M. M. Understanding catalytic mechanisms and cathode interface kinetics in nonaqueous Mg-CO_2 batteries. *ACS. Appl. Mater. Interfaces.* **2023**, *15*, 45895-904. DOI
39. Yang, C.; Guo, K.; Yuan, D.; Cheng, J.; Wang, B. Unraveling reaction mechanisms of Mo_2C as cathode catalyst in a Li-CO_2 battery. *J. Am. Chem. Soc.* **2020**, *142*, 6983-90. DOI
40. Jian, T.; Ma, W.; Hou, J.; Ma, J.; Xu, C.; Liu, H. From Ru to RuAl intermetallic/Ru heterojunction: Enabling high reversibility of the CO_2 redox reaction in Li-CO_2 battery based on lowered interface thermodynamic energy barrier. *Nano. Energy.* **2023**, *118*, 108998.

DOI

41. Hu, J.; Yang, C.; Guo, K. Understanding the electrochemical reaction mechanisms of precious metals Au and Ru as cathode catalysts in Li-CO_2 batteries. *J. Mater. Chem. A.* **2022**, *10*, 14028-40. DOI
42. Gupta, D.; Mao, J.; Guo, Z. Bifunctional catalysts for co_2 reduction and O_2 evolution: a pivotal for aqueous rechargeable Zn-CO_2 batteries. *Adv. Mater.* **2024**, *36*, e2407099. DOI
43. Pan, Q.; Ma, X.; Wang, H.; et al. Approaching splendid catalysts for Li-CO_2 battery from the theory to practical designing: a review. *Adv. Mater.* **2024**, *36*, e2406905. DOI
44. Guo, W.; Wang, Y.; Yi, Q.; et al. Research progress of aqueous Zn-CO_2 battery: design principle and development strategy of a multifunctional catalyst. *Front. Energy. Res.* **2023**, *11*, 1194674. DOI
45. Mu, X.; Pan, H.; He, P.; Zhou, H. Li-CO_2 and Na-CO_2 Batteries: toward greener and sustainable electrical energy storage. *Adv. Mater.* **2020**, *32*, e1903790. DOI
46. Cheng, Y.; Wang, Y.; Chen, B.; et al. Routes to bidirectional cathodes for reversible aprotic alkali metal-CO_2 batteries. *Adv. Mater.* **2024**, *36*, e2410704. DOI
47. Yue, J.; Zhang, J.; Tong, Y.; et al. Aqueous interphase formed by CO_2 brings electrolytes back to salt-in-water regime. *Nat. Chem.* **2021**, *13*, 1061-9. DOI
48. Liang, Y.; Yao, Y. Designing modern aqueous batteries. *Nat. Rev. Mater.* **2023**, *8*, 109-22. DOI
49. Gao, S.; Liu, Y.; Xie, Z.; et al. Metal-free bifunctional ordered mesoporous carbon for reversible Zn-CO_2 batteries. *Small. Methods.* **2021**, *5*, e2001039. DOI
50. Joseph, S.; Singh, G.; Lee, J. M.; et al. Hierarchical carbon structures from soft drink for multi-functional energy applications of Li-ion battery, Na-ion battery and CO_2 capture. *Carbon* **2023**, *210*, 118085. DOI
51. Larcher, D.; Tarascon, J. M. Towards greener and more sustainable batteries for electrical energy storage. *Nat. Chem.* **2015**, *7*, 19-29. DOI PubMed
52. Xiao, X.; Zhang, Z.; Tan, P. Unveiling the mysteries of operating voltages of lithium-carbon dioxide batteries. *Proc. Natl. Acad. Sci. USA.* **2023**, *120*, e2217454120. DOI PubMed PMC
53. Xu, L.; Liu, W.; Liu, K. Single atom environmental catalysis: influence of supports and coordination environments. *Adv. Funct. Mater.* **2023**, *33*, 2304468. DOI
54. Liang, S.; Huang, L.; Gao, Y.; Wang, Q.; Liu, B. Electrochemical reduction of CO_2 to CO over transition metal/N-doped carbon catalysts: the active sites and reaction mechanism. *Adv. Sci.* **2021**, *8*, e2102886. DOI PubMed PMC
55. Sarkar, A.; Dharmaraj, V. R.; Yi, C. H.; et al. Recent advances in rechargeable metal-CO_2 batteries with nonaqueous electrolytes. *Chem. Rev.* **2023**, *123*, 9497-564. DOI
56. Han, J.; Xu, Q.; Rong, J.; et al. Molecular engineering of porous Fe-N-C catalyst with sulfur incorporation for boosting CO_2 reduction and Zn-CO_2 battery. *Adv. Sci.* **2024**, *11*, e2407063. DOI PubMed PMC
57. Sun, X.; Mu, X.; Zheng, W.; et al. Binuclear Cu complex catalysis enabling Li-CO_2 battery with a high discharge voltage above 3.0 V . *Nat. Commun.* **2023**, *14*, 536. DOI PubMed PMC
58. Ci, L.; Song, L.; Jin, C.; et al. Atomic layers of hybridized boron nitride and graphene domains. *Nat. Mater.* **2010**, *9*, 430-5. DOI
59. Yang, S.; Qiao, Y.; He, P.; et al. A reversible lithium-CO_2 battery with Ru nanoparticles as a cathode catalyst. *Energy. Environ. Sci.* **2017**, *10*, 972-8. DOI
60. Guo, L.; Li, B.; Thirumal, V.; Song, J. Advanced rechargeable Na-CO_2 batteries enabled by a ruthenium@porous carbon composite cathode with enhanced Na_2CO_3 reversibility. *Chem. Commun.* **2019**, *55*, 7946-9. DOI
61. Xiao, X.; Tan, P.; Zhu, X.; Dai, Y.; Cheng, C.; Ni, M. Investigation on the discharge and charge behaviors of Li-CO_2 batteries with carbon nanotube electrodes. *ACS. Sustain. Chem. Eng.* **2020**, *8*, 9742-50. DOI
62. Sun, J.; Lu, Y.; Yang, H.; Han, M.; Shao, L.; Chen, J. Rechargeable Na-CO_2 batteries starting from cathode of Na_2CO_3 and carbon nanotubes. *Research* **2018**, *2018*, 6914626. DOI PubMed PMC
63. Kong, Y.; Gong, H.; Song, L.; Jiang, C.; Wang, T.; He, J. Nano-sized Au particle-modified carbon nanotubes as an effective and stable cathode for Li-CO_2 batteries. *Eur. J. Inorg. Chem.* **2021**, *2021*, 590-6. DOI
64. Yoo, E.; Zhou, H. Li-air rechargeable battery based on metal-free graphene nanosheet catalysts. *ACS. Nano.* **2011**, *5*, 3020-6. DOI PubMed
65. Xiao, J.; Mei, D.; Li, X.; et al. Hierarchically porous graphene as a lithium-air battery electrode. *Nano. Lett.* **2011**, *11*, 5071-8. DOI
66. Zhang, Z.; Zhang, Q.; Chen, Y.; et al. The first introduction of graphene to rechargeable Li-CO_2 batteries. *Angew. Chem. Int. Ed.* **2015**, *127*, 6650-3. DOI
67. Ye, F.; Gong, L.; Long, Y.; et al. Topological defect-rich carbon as a metal-free cathode catalyst for high-performance Li-CO_2 batteries. *Adv. Energy. Mater.* **2021**, *11*, 2101390. DOI
68. Yuan, C.; Li, H.; Jiang, Y.; et al. Tuning the activity of N-doped carbon for CO_2 reduction *via in situ* encapsulation of nickel nanoparticles into nano-hybrid carbon substrates. *J. Mater. Chem. A.* **2019**, *7*, 6894-900. DOI
69. Song, A.; Cao, L.; Yang, W.; et al. In situ construction of nitrogen-doped graphene with surface-grown carbon nanotubes as a multifactorial synergistic catalyst for oxygen reduction. *Carbon* **2019**, *142*, 40-50. DOI
70. Gottlieb, E.; Matyjaszewski, K.; Kowalewski, T. Polymer-based synthetic routes to carbon-based metal-free catalysts. *Adv. Mater.* **2019**, *31*, e1804626. DOI PubMed
71. Dong, Y.; Zhang, Q.; Tian, Z.; et al. Ammonia thermal treatment toward topological defects in porous carbon for enhanced carbon

dioxide electroreduction. *Adv. Mater.* **2020**, *32*, e2001300. DOI

72. Tan, G.; Chong, L.; Amine, R.; et al. Toward highly efficient electrocatalyst for Li-O_2 batteries using biphasic N-doping Cobalt@ Graphene multiple-capsule heterostructures. *Nano. Lett.* **2017**, *17*, 2959-66. DOI
73. Li, Y.; Zhou, J.; Zhang, T.; et al. Highly surface-wrinkled and N-doped CNTs anchored on metal wire: a novel fiber-shaped cathode toward high-performance flexible Li-CO_2 batteries. *Adv. Funct. Mater.* **2019**, *29*, 1808117. DOI
74. Xu, C.; Zhang, K.; Zhang, D.; et al. Reversible hybrid sodium-CO_2 batteries with low charging voltage and long-life. *Nano. Energy.* **2020**, *68*, 104318. DOI
75. Xu, C.; Zhan, J.; Wang, H.; Kang, Y.; Liang, F. Dense binary Fe-Cu sites promoting CO_2 utilization enable highly reversible hybrid Na-CO_2 batteries. *J. Mater. Chem. A.* **2021**, *9*, 22114-28. DOI
76. Chen, B.; Wang, D.; Zhang, B.; et al. Engineering the active sites of graphene catalyst: from CO_2 activation to activate Li-CO_2 batteries. *ACS. Nano.* **2021**, *15*, 9841-50. DOI
77. Li, X.; Qi, G.; Zhang, J.; Cheng, J.; Wang, B. Artificial solid-electrolyte interphase and bamboo-like N-doped carbon nanotube enabled highly rechargeable K-CO_2 batteries. *Adv. Funct. Mater.* **2022**, *32*, 2105029. DOI
78. Ma, G.; Ning, G.; Wei, Q. S-doped carbon materials: synthesis, properties and applications. *Carbon* **2022**, *195*, 328-40. DOI
79. Sun, T.; Huang, F.; Liu, J.; et al. Strengthened d-p orbital-hybridization of single atoms with sulfur species induced bidirectional catalysis for lithium-sulfur batteries. *Adv. Funct. Mater.* **2023**, *33*, 2306049. DOI
80. Dong, C.; Ma, C.; Zhou, C.; et al. Engineering d-p orbital hybridization with P, S Co-coordination asymmetric configuration of single atoms toward high-rate and long-cycling lithium-sulfur battery. *Adv. Mater.* **2024**, *36*, e2407070. DOI
81. Wang, G.; Liu, M.; Jia, J.; et al. Nitrogen and sulfur co-doped carbon nanosheets for electrochemical reduction of CO_2. *ChemCatChem* **2020**, *12*, 2203-8. DOI
82. Huang, K.; Li, R.; Qi, H.; et al. Regulating adsorption of intermediates via the sulfur modulating dual-atomic sites for boosting CO_2 RR. *ACS. Catal.* **2024**, *14*, 8889-98. DOI
83. Zhang, Z.; Bai, W.; Wang, K.; Chen, J. Electrocatalyst design for aprotic Li-CO_2 batteries. *Energy. Environ. Sci.* **2020**, *13*, 4717-37. DOI
84. Balu, S.; Hanan, A.; Venkatesvaran, H.; Chen, S.; Yang, T. C.; Khalid, M. Recent progress in surface-defect engineering strategies for electrocatalysts toward electrochemical CO_2 reduction: a review. *Catalysts* **2023**, *13*, 393. DOI
85. Wang, Y.; Cheng, Y.; Chen, B.; et al. p-band regulation guides the free-standing porous carbon electrode for efficient Na-CO_2 batteries. *Energy. Storage. Mater.* **2024**, *71*, 103655. DOI
86. Song, L.; Hu, C.; Xiao, Y.; et al. An ultra-long life, high-performance, flexible Li-CO_2 battery based on multifunctional carbon electrocatalysts. *Nano. Energy.* **2020**, *71*, 104595. DOI
87. Qie, L.; Lin, Y.; Connell, J. W.; Xu, J.; Dai, L. Highly rechargeable lithium-CO_2 batteries with a boron- and nitrogen-codoped holey-graphene cathode. *Angew. Chem. Int. Ed.* **2017**, *56*, 6970-4. DOI PubMed
88. Kaur, S.; Kumar, M.; Gupta, D.; et al. Efficient CO_2 utilization and sustainable energy conversion via aqueous Zn-CO_2 batteries. *Nano. Energy.* **2023**, *109*, 108242. DOI
89. Gao, M.; Li, C.; Wang, R.; Xiao, S.; Guo, Z.; Wang, Y. Noble metal catalysts for metal-air batteries: from nano-level to atom-level. *Next. Mater.* **2024**, *2*, 100126. DOI
90. Yu, A.; Liu, S.; Zhang, W.; Yang, Y. Molten salt electrolytic CO_2-derived carbon-based nanomaterials for energy storage and electrocatalysis: a review. *ACS. Appl. Nano. Mater.* **2024**, *7*, 27960-78. DOI
91. Wang, F.; Shang, S.; Li, Z.; Zhang, Z.; Chu, K. Selective urea electrosynthesis from nitrate and CO_2 on isolated copper alloyed ruthenium. *ACS. Energy. Lett.* **2024**, *9*, 4624-32. DOI
92. Liu, Z.; Ma, J.; Guo, Y.; Hong, M.; Sun, R. Photocatalytic CO_2 reduction integrated with biomass selective oxidation via single-atom Ru and P dual sites on carbon nitride. *Appl. Catal. B. Environ.* **2024**, *342*, 123429. DOI
93. Qiao, Y.; Yi, J.; Wu, S.; et al. Li-CO_2 electrochemistry: a new strategy for CO_2 fixation and energy storage. *Joule* **2017**, *1*, 359-70. DOI
94. Lin, J.; Ding, J.; Wang, H.; et al. Boosting energy efficiency and stability of Li-CO_2 batteries via synergy between Ru atom clusters and single-atom Ru-N_4 sites in the electrocatalyst cathode. *Adv. Mater.* **2022**, *34*, e2200559. DOI
95. Thoka, S.; Tsai, C. M.; Tong, Z.; et al. Comparative study of Li-CO_2 and Na-CO_2 batteries with Ru@CNT as a cathode catalyst. *ACS. Appl. Mater. Interfaces.* **2021**, *13*, 480-90. DOI
96. Zhao, J.; Xu, X.; Chen, J.; et al. Ultrafine Ru nanoparticles anchored on N-doped mesoporous hollow carbon spheres as a highly efficient bifunctional catalyst for Li-CO_2 batteries. *J. Power. Sources.* **2024**, *607*, 234577. DOI
97. Lian, Z.; Lu, Y.; Wang, C.; et al. Single-atom Ru implanted on Co_3O_4 nanosheets as efficient dual-catalyst for Li-CO_2 batteries. *Adv. Sci.* **2021**, *8*, 2102550. DOI PubMed PMC
98. Xu, C.; Qiu, J.; Dong, Y.; et al. Dual-functional electrode promoting dendrite-free and CO_2 utilization enabled high-reversible symmetric Na-CO_2 batteries. *Energy. Environ. Mater.* **2024**, *7*, e12626. DOI
99. Chen, S.; Yang, K.; Zhu, H.; et al. Rational catalyst structural design to facilitate reversible Li-CO_2 batteries with boosted CO_2 conversion kinetics. *Nano. Energy.* **2023**, *117*, 108872. DOI
100. Rho, Y.; Yoo, Y. J.; Ryu, W. Research trends on minimizing the size of noble metal catalysts for Li-CO_2 batteries: from nanoparticle to single atom. *Korean. J. Chem. Eng.* **2023**, *40*, 461-72. DOI
101. Najafli, E.; Ratso, S.; Foroozan, A.; Noor, N.; Higgins, D. C.; Kruusenberg, I. Functionalization of CO_2-derived carbon support as a

pathway to enhancing the oxygen reduction reaction performance of Pt electrocatalysts. *Energy. Fuels.* **2024**, *38*, 15601-10. DOI

102. Chen, Z.; Yuan, M.; Tang, Z.; Zhu, H.; Zeng, G. Magnetron sputtering of platinum on nitrogen-doped polypyrrole carbon nanotubes as an efficient and stable cathode for lithium-carbon dioxide batteries. *Phys. Chem. Chem. Phys.* **2023**, *25*, 7662-8. DOI
103. Zhang, P. F.; Zhuo, H. Y.; Dong, Y. Y.; et al. Pt nanoparticles confined in a 3D porous FeNC matrix as efficient catalysts for rechargeable Li-CO_2/O_2 batteries. *ACS. Appl. Mater. Interfaces.* **2023**, *15*, 2940-50. DOI
104. Xing, Y.; Yang, Y.; Li, D.; et al. Crumpled Ir nanosheets fully covered on porous carbon nanofibers for long-life rechargeable lithium-CO_2 batteries. *Adv. Mater.* **2018**, *30*, e1803124. DOI
105. Gu, Y.; Liu, B.; Zeng, X.; et al. A flexible Li-CO_2 batteries with enhanced cycling stability enabled by a IrO_2/carbon fiber self-standing cathode. *Electrochim. Acta.* **2023**, *443*, 141951. DOI
106. Wu, G.; Li, X.; Zhang, Z.; et al. Design of ultralong-life Li-CO_2 batteries with IrO_2 nanoparticles highly dispersed on nitrogen-doped carbon nanotubes. *J. Mater. Chem. A.* **2020**, *8*, 3763-70. DOI
107. Ma, W.; Liu, X.; Li, C.; et al. Rechargeable Al-CO_2 batteries for reversible utilization of CO_2. *Adv. Mater.* **2018**, *30*, e1801152. DOI
108. Bagchi, D.; Sarkar, S.; Singh, A. K.; Vinod, C. P.; Peter, S. C. Potential- and time-dependent dynamic nature of an oxide-derived PdIn nanocatalyst during electrochemical CO_2 reduction. *ACS. Nano.* **2022**, *16*, 6185-96. DOI PubMed
109. Zhuang, Q.; Hu, C.; Zhu, W.; et al. Facile synthesis of MnO/NC nanohybrids toward high-efficiency ORR for zinc-air battery. *RSC. Adv.* **2024**, *14*, 24031-8. DOI PubMed PMC
110. Yang, M.; Liu, S.; Sun, J.; et al. Highly dispersed Bi clusters for efficient rechargeable Zn-CO_2 batteries. *Appl. Catal. B. Environ.* **2022**, *307*, 121145. DOI
111. Naik, K. M.; Kumar, C. A.; Sharma, C. S. Nano-interface engineering of $NiFe_2O_4$/MoS_2/MWCNTs heterostructure catalyst as cathodes in the long-life reversible Li-CO_2 mars batteries. *Chem. Eng. J.* **2024**, *490*, 151729. DOI
112. Peng, M.; Ci, S.; Shao, P.; Cai, P.; Wen, Z. Cu_3P/C nanocomposites for efficient electrocatalytic CO_2 reduction and Zn-CO_2 battery. *J. Nanosci. Nanotechnol.* **2019**, *19*, 3232-6. DOI
113. Zheng, W.; Yang, J.; Chen, H.; et al. Atomically defined undercoordinated active sites for highly efficient CO_2 electroreduction. *Adv. Funct. Mater.* **2020**, *30*, 1907658. DOI
114. Liu, Y.; Shu, P.; Zhang, M.; et al. Uncovering the geometry activity of spinel oxides in Li-CO_2 battery reactions. *ACS. Energy. Lett.* **2024**, *9*, 2173-81. DOI
115. Xu, C.; Zhan, J.; Wang, Z.; et al. Biomass-derived highly dispersed Co/Co_9S_8 nanoparticles encapsulated in S, N-co-doped hierarchically porous carbon as an efficient catalyst for hybrid Na-CO_2 batteries. *Mater. Today. Energy.* **2021**, *19*, 100594. DOI
116. Liu, B.; Sun, Y.; Liu, L.; Xu, S.; Yan, X. Advances in manganese-based oxides cathodic electrocatalysts for Li-air batteries. *Adv. Funct. Mater.* **2018**, *28*, 1704973. DOI
117. Bai, L.; Duan, Z.; Wen, X.; Si, R.; Guan, J. Atomically dispersed manganese-based catalysts for efficient catalysis of oxygen reduction reaction. *App. Catal. B. Environ.* **2019**, *257*, 117930. DOI
118. Wang, H.; Yang, Y.; Liu, J.; et al. The role of manganese-based catalyst in electrocatalytic water splitting: recent research and progress. *Mater. Today. Phy.* **2023**, *36*, 101169. DOI
119. Liu, L.; Shen, S.; Zhao, N.; et al. Revealing the indispensable role of in situ electrochemically reconstructed Mn(II)/Mn(III) in improving the performance of lithium-carbon dioxide batteries. *Adv. Mater.* **2024**, *36*, e2403229. DOI
120. Wang, S.; Wang, L.; Wang, D.; Li, Y. Recent advances of single-atom catalysts in CO_2 conversion. *Energy. Environ. Sci.* **2023**, *16*, 2759-803. DOI
121. Dai, Y.; Li, H.; Wang, C.; et al. Manipulating local coordination of copper single atom catalyst enables efficient CO_2-to-CH_4 conversion. *Nat. Commun.* **2023**, *14*, 3382. DOI PubMed PMC
122. Zhang, Y.; Johannessen, B.; Zhang, P.; Gong, J.; Ran, J.; Qiao, S. Z. Reversed Electron transfer in dual single atom catalyst for boosted photoreduction of CO_2. *Adv. Mater.* **2023**, *35*, e2306923. DOI PubMed
123. Miao, K.; Qin, J.; Yang, J.; Kang, X. Synergy of Ni nanoclusters and single atom site: size effect on the performance of electrochemical CO_2 reduction reaction and rechargeable Zn-CO_2 batteries. *Adv. Funct. Mater.* **2024**, *34*, 2316824. DOI
124. Li, H.; Pan, F.; Qin, C.; Wang, T.; Chen, K. Porous organic polymers-based single-atom catalysts for sustainable energy-related electrocatalysis. *Adv. Energy. Mater.* **2023**, *13*, 2301378. DOI
125. Zhang, W.; Zhang, J.; Wang, N.; et al. Two-electron redox chemistry via single-atom catalyst for reversible zinc-air batteries. *Nat. Sustain.* **2024**, *7*, 463-73. DOI
126. Bao, Y.; Xiao, J.; Huang, Y.; et al. Regulating spin polarization via axial nitrogen traction at Fe-N_5 sites enhanced electrocatalytic CO_2 reduction for Zn-CO_2 batteries. *Angew. Chem. Int. Ed.* **2024**, *63*, e202406030. DOI
127. Xu, Y.; Gong, H.; Song, L.; et al. A highly efficient and free-standing copper single atoms anchored nitrogen-doped carbon nanofiber cathode toward reliable Li-CO_2 batteries. *Mater. Today. Energy.* **2022**, *25*, 100967. DOI
128. Zhu, K.; Li, X.; Choi, J.; et al. Single-Atom Cadmium-N_4 sites for rechargeable Li-CO_2 batteries with high capacity and ultra-long lifetime. *Adv. Funct. Mater.* **2023**, *33*, 2213841. DOI
129. Li, J.; Chen, L.; Hao, Y.; et al. Asymmetric coordinated single-atom Pd sites for high performance CO_2 electroreduction and Zn-CO_2 battery. *Chem. Eng. J.* **2023**, *461*, 141865. DOI
130. Sun, X.; Hou, Z.; He, P.; Zhou, H. Recent advances in rechargeable Li-CO_2 batteries. *Energy. Fuels.* **2021**, *35*, 9165-86. DOI
131. Li, S.; Dong, Y.; Zhou, J.; et al. Carbon dioxide in the cage: manganese metal-organic frameworks for high performance CO_2 electrodes in Li-CO_2 batteries. *Energy. Environ. Sci.* **2018**, *11*, 1318-25. DOI

132. Li, S.; Liu, Y.; Zhou, J.; et al. Monodispersed MnO nanoparticles in graphene-an interconnected N-doped 3D carbon framework as a highly efficient gas cathode in Li-CO_2 batteries. *Energy. Environ. Sci.* **2019**, *12*, 1046-54. DOI
133. Li, W.; Zhang, M.; Sun, X.; et al. Boosting a practical Li-CO_2 battery through dimerization reaction based on solid redox mediator. *Nat. Commun.* **2024**, *15*, 803. DOI PubMed PMC
134. Lu, M.; Zhang, M.; Liu, J.; et al. Covalent organic framework based functional materials: important catalysts for efficient CO_2 utilization. *Angew. Chem. Int. Ed.* **2022**, *134*, e202200003. DOI
135. Sun, C.; Sheng, D.; Wang, B.; Feng, X. Covalent organic frameworks for extracting water from air. *Angew. Chem. Int. Ed.* **2023**, *135*, e202303378. DOI
136. Nguyen, H. L.; Gropp, C.; Hanikel, N.; Möckel, A.; Lund, A.; Yaghi, O. M. Hydrazine-hydrazide-linked covalent organic frameworks for water harvesting. *ACS. Cent. Sci.* **2022**, *8*, 926-32. DOI PubMed PMC
137. Li, X.; Wang, H.; Chen, Z.; et al. Covalent-organic-framework-based Li-CO_2 batteries. *Adv. Mater.* **2019**, *31*, e1905879. DOI
138. Zhang, Y.; Zhong, R. L.; Lu, M.; et al. Single Metal site and versatile transfer channel merged into covalent organic frameworks facilitate high-performance Li-CO_2 batteries. *ACS. Cent. Sci.* **2021**, *7*, 175-82. DOI PubMed PMC
139. Lin, R.; Chen, B. Hydrogen-bonded organic frameworks: chemistry and functions. *Chem* **2022**, *8*, 2114-35. DOI
140. Yin, Q.; Alexandrov, E. V.; Si, D. H.; et al. Metallization-prompted robust porphyrin-based hydrogen-bonded organic frameworks for photocatalytic CO_2 reduction. *Angew. Chem. Int. Ed.* **2022**, *61*, e202115854. DOI
141. Lin, Z. J.; Mahammed, S. A. R.; Liu, T. F.; Cao, R. Multifunctional porous hydrogen-bonded organic frameworks: current status and future perspectives. *ACS. Cent. Sci.* **2022**, *8*, 1589-608. DOI PubMed PMC
142. Karmakar, A.; Illathvalappil, R.; Anothumakkool, B.; et al. Hydrogen-bonded organic frameworks (HOFs): a new class of porous crystalline proton-conducting materials. *Angew. Chem. Int. Ed.* **2016**, *55*, 10667-71. DOI
143. Yang, Y.; Li, L.; Lin, R. B.; et al. Ethylene/ethane separation in a stable hydrogen-bonded organic framework through a gating mechanism. *Nat. Chem.* **2021**, *13*, 933-9. DOI
144. Zhang, Z.; Ye, Y.; Xiang, S.; Chen, B. Exploring multifunctional hydrogen-bonded organic framework materials. *ACC. Chem. Res.* **2022**, *55*, 3752-66. DOI
145. Chen, L.; Yuan, Z.; Zhang, H.; et al. A flexible hydrogen-bonded organic framework constructed from a tetrabenzaldehyde with a carbazole N-H binding site for the highly selective recognition and separation of acetone. *Angew. Chem. Int. Ed.* **2022**, *61*, e202213959. DOI
146. Guo, C.; Han, B.; Sun, W.; Cao, Y.; Zhang, Y.; Wang, Y. Hydrogen-bonded organic framework for high-performance lithium/sodium-iodine organic batteries. *Angew. Chem. Int. Ed.* **2022**, *61*, e202213276. DOI
147. Cheng, Z.; Fang, Y.; Yang, Y.; et al. Hydrogen-bonded organic framework to upgrade cycling stability and rate capability of Li-CO_2 batteries. *Angew. Chem. Int. Ed.* **2023**, *135*, e202311480. DOI
148. Hao, X.; An, X.; Patil, A. M.; et al. Biomass-derived N-doped carbon for efficient electrocatalytic CO_2 reduction to CO and Zn-CO_2 batteries. *ACS. Appl. Mater. Interfaces.* **2021**, *13*, 3738-47. DOI
149. Chen, J.; Wang, Y.; Li, S.; et al. Porous metal current collectors for alkali metal batteries. *Adv. Sci.* **2022**, *10*, e2205695. DOI PubMed PMC
150. Xiao, Y.; Du, F.; Hu, C.; et al. High-performance Li-CO_2 batteries from free-standing, binder-free, bifunctional three-dimensional carbon catalysts. *ACS. Energy. Lett.* **2020**, *5*, 916-21. DOI
151. Yang, H.; Lin, Q.; Wu, Y.; et al. Highly efficient utilization of single atoms via constructing 3D and free-standing electrodes for CO_2 reduction with ultrahigh current density. *Nano. Energy.* **2020**, *70*, 104454. DOI
152. Zhou, J.; Cheng, J.; Wang, B.; Peng, H.; Lu, J. Flexible metal-gas batteries: a potential option for next-generation power accessories for wearable electronics. *Energy. Environ. Sci.* **2020**, *13*, 1933-70. DOI
153. Chen, L.; Zhou, J.; Wang, Y.; et al. Flexible, stretchable, water-/fire-proof fiber-shaped Li-CO_2 batteries with high energy density. *Adv. Energy. Mater.* **2023**, *13*, 2202933. DOI
154. Hu, T.; Hu, Y.; Yao, T.; et al. Freestanding molybdenum carbide nanowires electrode for high specific capacity and superior rate performance Li-CO_2 batteries. *Energy. Storage. Mater.* **2024**, *72*, 103740. DOI
155. Chen, M.; Liu, Y.; Liang, X.; Wang, F.; Li, Y.; Chen, Q. Integrated carbon nanotube/MoO_3 core/shell arrays as freestanding air cathodes for flexible Li-CO_2 batteries. *Energy. Technol.* **2021**, *9*, 2100547. DOI
156. Cheng, Z.; Wu, Z.; Chen, J.; et al. Mo_2N-ZrO_2 heterostructure engineering in freestanding carbon nanofibers for upgrading cycling stability and energy efficiency of Li-CO_2 batteries. *Small* **2023**, *19*, e2301685. DOI
157. Zhao, W.; Yang, Y.; Deng, Q.; et al. Toward an understanding of bimetallic MXene solid-solution in binder-free electrocatalyst cathode for advanced Li-CO_2 batteries. *Adv. Funct. Mater.* **2023**, *33*, 2210037. DOI
158. Liu, L.; Qin, Y.; Zhao, H.; et al. Suppression of CO_2 induced lithium anode corrosion by fluorinated functional group in quasi-solid polymer electrolyte enabling long-cycle and high-safety Li-CO_2 batteries. *Energy. Storage. Mater.* **2023**, *57*, 260-8. DOI
159. Wang, F.; Li, Y.; Xia, X.; Cai, W.; Chen, Q.; Chen, M. Metal-CO_2 electrochemistry: from CO_2 recycling to energy storage. *Adv. Energy. Mater.* **2021**, *11*, 2100667. DOI
160. Zhang, P.; Chen, Z.; Shang, N.; et al. Advances in polymer electrolytes for solid-state zinc-air batteries. *Mater. Chem. Front.* **2023**, *7*, 3994-4018. DOI
161. Xu, S.; Das, S. K.; Archer, L. A. The Li-CO_2 battery: a novel method for CO_2 capture and utilization. *RSC. Adv.* **2013**, *3*, 6656. DOI
162. Zhu, K.; Li, X.; Choi, J.; et al. Single-atom cadmium-N_4 sites for rechargeable Li-CO_2 batteries with high capacity and ultra-long

lifetime. *Adv. Funct. Mater.* **2023**, *33*, 2213841. DOI

163. Hu, X.; Li, Z.; Zhao, Y.; et al. Quasi-solid state rechargeable Na-CO_2 batteries with reduced graphene oxide Na anodes. *Sci. Adv.* **2017**, *3*, e1602396. DOI PubMed PMC
164. Xu, S.; Lu, Y.; Wang, H.; Abruña, H. D.; Archer, L. A. A rechargeable Na-CO_2/O_2 battery enabled by stable nanoparticle hybrid electrolytes. *J. Mater. Chem. A.* **2014**, *2*, 17723-9. DOI
165. Zhang, W.; Hu, C.; Guo, Z.; Dai, L. High-performance K-CO_2 batteries based on metal-free carbon electrocatalysts. *Angew. Chem. Int. Ed.* **2020**, *59*, 3470-4. DOI
166. Sadat WI, Archer LA. The O_2-assisted Al/CO_2 electrochemical cell: a system for CO_2 capture/conversion and electric power generation. *Sci. Adv.* **2016**, *2*, e1600968. DOI PubMed PMC